140
42

PHASE-EQUILIBRIA OF SOME BINARY SYSTEMS AT LOW TEMPERATURES

M. H. OMAR

STELLINGEN

I

The relatively high value for the solubility of nitrogen in hydrogen at 20°K, which has been measured by **Petit**, is probably due to the adsorption of hydrogen on the metal part of his analysis apparatus, which was immersed in liquid hydrogen.

Petit, P., Thesis, University of Grenoble 1959.
Weil, L. and Petit, P., Proc. of the Meeting of Commission I of the Internat. Inst. of Refrig., Delft, 1958.

II

The suggestion of **Fedorova**, which was based on the analysis of heat-capacity measurements, concerning the formation of an intermediate condensed phase in the N_2–CH_4 system is excluded by our measurements.

Fedorova, M. F., J. Expt. Theoret. Phys. U.S.S.R. 8 (1938) 425.
Chapter II, this thesis.

III

The measurements of **Yunker** and **Halsey** on the solid-liquid phase equilibrium of the Ar–Xe system are in error.

Yunker, W. H. and Halsey, G. D. Jr., J. Phys. Chem. 64 (1960) 484.
Heastie, R. and Lefebvre, C., Proc. phys. Soc. 76 (1960) 180.

IV

Fastovsky and **Krestinsky** inadequately performed some calculations on the solubility of methane in liquid nitrogen and tried to compare these calculations with their experimental measurements.

Fastovsky, V. G. and Krestinsky, Yu. A., J. Phys. Chem. U.S.S.R. 15 (1941) 525.

STELLINGEN

I

The relatively high value for the solubility of nitrogen in hydrogen at 20°K, which has been measured by Petit, is probably due to the adsorption of hydrogen on the metal part of his analysis apparatus, which was immersed in liquid hydrogen.

Petit, P., Thesis, University of Grenoble 1959.
Weil, L. and Petit, P., Proc. of the Meeting of Commission I of the Internat. Inst. of Refrig., Delft, 1958.

II

The suggestion of Fedorova, which was based on the analysis of heat-capacity measurements, concerning the formation of an intermediate condensed phase in the N_2–CH_4 system is excluded by our measurements.

Fedorova, M. F., J. expt. theort. Phys. U.S.S.R. **8** (1938) 425.
Chapter II, this thesis.

III

The measurements of Yunker and Halsey on the solid-liquid phase equilibrium of the Ar–Xe system are in error.

Yunker, W. H. and Halsey, G. D. Jr., J. Phys. Chem. **64** (1960) 484.
Heastie, R. and Lefèbvre, C., Proc. phys. Soc. **76** (1960) 180.

IV

Fastovsky and Krestinsky inadequately performed some calculations on the solubility of methane in liquid nitrogen and tried to compare these calculations with their experimental measurements.

Fastovsky, V. G. and Krestinsky, Y. A., J. Phys. Chem. U.S.S.R. **15** (1941) 525.

V

The p–x diagram given by Kirkwood and Oppenheim to illustrate the partial pressures for a binary system with positive deviation from ideality is not correct.

Kirkwood, J. G. and Oppenheim, I., "Chemical Thermodynamics", Mc-Graw Hill Book Company, Inc. N.Y. 1961. fig. 9-15, p. 140.

VI

To eliminate inconsistencies in published data for the 100-yard sprint in athletics, it is necessary to indicate the possible errors in the measurements.

The Times 21st. July 1958.

VII

The assertion of Brewer and Keyston that the addition of 0.066% ^{4}He to ^{3}He could cause phase separation at 0.15°K is doubtful.

Brewer, D. F. and Keyston, I. R. G., Physics Letters **1** (1962) 5.

VIII

Some transactions of the religion of Islam. such as marriage laws and women's rights, which are sometimes misunderstood in the western world, could best be clarified through a series of publications to be issued by an authorized Islamic centre, such as Al-Azhar University in Cairo.

IX

When applying the method proposed by Bragg for measuring the temperature of fluids, using the principle of cavitating venturi, an appropriate correction should be applied to account for the expansion of the liquid.

I. E. Smith "Progress in Cryogenics" edited by K. Mendelsohn Heywood and Company Ltd. London (1961). Vol. 3, chapt IV.

X

Helium gas is frequently used for the pressurization of cryogenic propellants in rocket engine systems; the determination of the solubility of helium in liquid oxygen would show if the dissolved helium has any influence on the working conditions of the rocket engines.

V

The p-x diagram given by Kirkwood and Oppenheim to illustrate the partial pressures for a binary system with positive deviation from ideality is not correct.

Kirkwood, J. G. and Oppenheim, I., "Chemical Thermodynamics", McGraw Hill Book Company, Inc. N.Y. 1961, fig. 9-12, p. 140.

VI

To eliminate inconsistencies in published data for the 100-yard sprint in athletics, it is necessary to indicate the possible errors in the measurements.

The Times 21st. July 1958

VII

The assertion of Brewer and Keyston that the addition of 0.085% ^{3}He to ^{4}He would cause phase separation at 0.15°K is doubtful.

Brewer, D. F. and Keyston, J. R. G., Physics Letters 1 (1962) 5.

VIII

Some injunctions of the religion of Islam, such as marriage laws and women's rights, which are sometimes misunderstood in the western world, could best be clarified through a series of publications to be issued by an authorized Islamic centre, such as Al-Azhar University in Cairo.

IX

When applying the method proposed by Bragg for measuring the temperature of fluids, using the principle of vibrating needles, an appropriate correction should be applied to account for the expansion of the liquid.

J. S. Smith, "Progress in Cryogenics", edited by K. Mendelssohn, Heywood and Company Ltd. London (1960), Vol. 2, Chapt. IV.

X

Helium gas is frequently used for the pressurization of cryogenic propellants in rocket engine systems. The determination of the solubility of helium in liquid oxygen would show if the dissolved helium has any influence on the working conditions of the rocket engines.

PHASE-EQUILIBRIA OF SOME BINARY SYSTEMS AT LOW TEMPERATURES

PHASE-EQUILIBRIA OF SOME BINARY SYSTEMS AT LOW TEMPERATURES

PROEFSCHRIFT

TER VERKRIJGING VAN DE GRAAD VAN DOCTOR IN
DE WIS- EN NATUURKUNDE AAN DE RIJKSUNIVERSITEIT TE LEIDEN, OP GEZAG VAN DE RECTOR
MAGNIFICUS DR. G. SEVENSTER, HOOGLERAAR IN
DE FACULTEIT DER GODGELEERDHEID, TEGEN DE
BEDENKINGEN VAN DE FACULTEIT DER WIS- EN
NATUURKUNDE TE VERDEDIGEN OP
WOENSDAG 27 JUNI 1962 TE 15 UUR

DOOR

MOHAMMED HOSNY OMAR

GEBOREN TE ELMANZALAH DAQUAHLIYAH, EGYPTE
IN 1935

Promotor: PROF. DR. K. W. TACONIS

Dit proefschrift is bewerkt onder leiding van Dr. Z. DOKOUPIL

TO MY PARENTS

Promotor: Prof. Dr. K. W. Taconis

Dit proefschrift is bewerkt onder leiding van Dr. Z. Dokoupil

On request of the Faculty of Science, here follows a short account of my academic studies:

My early education took place in Elmanzalah-Daquahliyah (northern part of Egypt), where I was born. Ending the high school in 1952, I started my study at the Faculty of Science, Ain-Shams University (Cairo), with the subjects: physics, mathematics, chemistry, and geology. In 1957, I obtained the Bachelor of Sciences (B.Sc.), the special degree in physics, with distinction.

I worked for about a year as assistant in the department of physics in the same university.

A mission-membership for the University of Assyout (southern part of Egypt) brought me in 1958 to the Kamerlingh Onnes Laboratory at Leiden to study for the doctors degree in experimental physics at low temperatures.

During my first year in this laboratory I assisted in some different types of experiments, meanwhile, I was preparing for the Doctoraal degree.

After passing examinations by prof. S. R. de Groot, and by prof. K. W. Taconis, I got the Doctoraal degree in experimental physics from Leiden University in 1960. Miss H. G. M. Schroten assisted me since 1961.

CONTENTS

INTRODUCTION 1

CHAPTER I. *Some supplementary measurements on the vapour-liquid equilibrium of the system hydrogen-nitrogen at temperatures higher than the triple point of nitrogen* 4
1. Introduction 4
2. Experimental procedure 5
3. Results 6
4. Thermodynamical analysis 10

CHAPTER II. *Determination of the solid-liquid equilibrium diagram for the nitrogen-methane system* 15
1. Introduction 15
2. The three-dimensional model of the N_2–CH_4 system 16
3. Experimental methods used for the determination of the melting diagram of the system N_2–CH_4 19
   A. Heat capacity method 20
   B. The thermal method 20
   C. Vapour pressure method 21
4. Apparatus and experimental procedure 22
5. Experimental results 24
6. Discussion 30

CHAPTER III. *Solid-gas equilibrium of the binary oxygen-hydrogen system* 36
1. Introduction 36
2. Experimental method 37
3. Results 38
4. Discussion 41

CHAPTER IV. *Solubility of nitrogen and oxygen in liquid hydrogen at temperatures between* 27 *and* 33°K 43
1. Introduction 43
2. Phase-equilibrium behaviour 44
3. Experimental method 45
4. Experimental results 47
5. Discussion of the results 49

ACKNOWLEDGEMENTS 53

SAMENVATTING 54

INTRODUCTION

The coexistence of matter in the different states of aggregation: gas, liquid, or solid, underlines the basics of the phase-equilibrium theory. It is not only pure components which can exhibit the above mentioned states of aggregation, but also mixtures are subject to similar phase changes. Usually, one represents the phase equilibrium data for binary mixtures either on a *p–x*-diagram giving the variation of the pressure with concentration at a given temperature, or on a *T–x*-diagram giving the variation of temperature with concentration at a constant pressure. The phase behaviour of almost all pure substances is known by now. Various phase-diagrams for binary or multicomponent-systems of metals are known to metallurgists. Geologists have investigated the phase behaviour of several minerals. Extensive studies concerning the phase equilibria of mixtures of substances have been carried out in chemistry. The majority of the above investigations are done at room or high temperatures.

When low temperatures became available it was natural to extend such studies to systems coexisting in equilibrium at low temperatures. On lowering the temperature sufficiently the so-called permanent gases can be transformed into the liquid or the solid phases. Consequently, it was interesting to study the various types of phase-equilibria for mixtures of these gases. The main investigated equilibria in such cases were: gas-liquid, gas-solid and solid-liquid. The solid-liquid equilibrium may result in cases where a liquid mixture can be in equilibruim with a solid phase consisting of the pure components only, or the liquid mixture in equilibrium with a solid formed of mixed crystals; it is also possible to have a liquid mixture in equilibrium with a solid phase which is of an intermediate type between the previous two cases. The liquid-liquid phase-equilibrium for condensed gas mixtures was not found in earlier studies, but was recently encountered for the binary mixtures: ^{3}He–^{4}He and O_2–O_3. The solid-solid phase equilibrium of solidified gas mixtures has not yet received much attention.

To investigate these various types of equilibria at low temperatures the different experimental methods and procedures applied at moderate or high temperatures may be adapted with some modification for low temperature work. In some cases it is necessary to develop special experimental techniques. For instance, special analyzing procedures are needed frequently for the detection of very low gas concentrations while working with the solid-gas phase equilibria.

When the data on phase equilibria are obtainable over a sufficiently large p–T–x range, it will be possible to construct a three-dimensional phase equilibrium model for a given binary system. Such equilibrium models are useful for the locations of the boundaries between the different types of phase equilibria, and also can help much to understand the behaviour of the given system under different p, T, and x-conditions.

The existance of experimental data on low temperature phase-equilibria for mixtures of gases is important for many reasons. From the point of view of thermodynamics it is desirable to check the thermodynamic consistency of such data and, in some cases, appropriate thermodynamic relations can be applied for the intrapolation and the smoothing of the data.

The determination of some important parameters such as virial coefficients or interaction energy parameters from accurate equilibrium data is valuable for testing the validity of the molecular theories of mixtures; sometimes phase-equilibrium data can be used successfully to evaluate these parameters when direct methods are experimentally not applicable.

It is also of great importance for cryogenic engineers to have accurate data concernig phase equilibria at low temperatures when designing low-temperature plants for separation, purification, or liquefaction of gases.

It was our purpose to carry out some work representing different types of phase equilibria for binary systems of some important technical gases. In addition, we have discussed our measurements, and the corresponding thermodynamic calculations were performed.

In this thesis, the following phase equilibria have been studied: H_2–N_2 vapour-liquid, N_2–CH_4 liquid-solid, H_2–O_2 gas-solid and finally the solubility of nitrogen and oxygen in hydrogen at liquid hydrogen temperatures. The various apparatus and experimental methods used to investigate these equilibria are also described.

Chapter I deals with the vapour-liquid equilibrium of the hydrogen-nitrogen system at temperatures between 63–74°K, and under pressures varying between 5 and 45 atm. These results were obtained using the flow method. Analysis of the vapour sample was done by freezing out the nitrogen at 20°K. A thermodynamic treatment using the Gibbs-Duhem relation is worked out and is applied with success to this system. The Beattie-Bridgeman equation of state, limited up to the second virial coefficient, proved to describe satisfactorily the vapour phase in the p–T range of our measurements. A graphical method is proposed to extrapolate the dew-curves at low pressures down to the vapour pressure of nitrogen.

The solid-liquid equilibrium of the binary N_2–CH_4 system is described in chapter II. The melting diagram of this system was determined using a combined method comprising measurements of vapour pressure, thermal analysis, and heat capacity of the condensed mixtures. A survey of earlier work on similar equilibrium of binary condensed mixtures of gases is included, and a brief account on the experimental methods used is also given. A three-dimensional phase equilibrium model for the N_2–CH_4 system is constructed in the neighbourhood of the triple-point temperatures. The behaviour of the melting diagram is treated thermodynamically on the basis of the regular solution theory.

The gas-solid equilibrium of the system H_2–O_2 is presented in chapter III. The measurements were carried out at temperatures between 40–54°K, and under pressures of 5, 10, and 15 atm. The experimental results are in good agreement with the theory developed by Dokoupil which was applied with success to similar equilibrium.

The last chapter, IV, deals with the solubility of nitrogen and oxygen in liquid hydrogen at temperatures below the critical point of hydrogen down to about 27°K. The measurements were carried out at pressures slightly higher than the vapour pressure of hydrogen. A modified static method was used to avoid the blockage of the inlet capillary with solid nitrogen or solid oxygen. The solubility theory of Hildebrand was applied to these systems, and the solubility parameter term $(\delta_1 - \delta_2)$ was calculated from the experimental results.

CHAPTER I

SOME SUPPLEMENTARY MEASUREMENTS ON THE VAPOUR-LIQUID EQUILIBRIUM OF THE SYSTEM HYDROGEN-NITROGEN AT TEMPERATURES HIGHER THAN THE TRIPLE POINT OF NITROGEN

Summary

The equilibrium between the liquid and gas phases of mixtures of hydrogen and nitrogen has been studied using the flow method. The working pressures were 5, 10, 15, 25, 35 and 45 atm at the temperatures of 63.1, 68.1, 72.3 and 74.6°K. A graphical method is described to extrapolate the dew curves to very low pressures. A thermodynamical treatment correlating the dew and boiling points is discussed.

1. *Introduction.* One can summarize the work done on the low temperature phase equilibrium of the system hydrogen-nitrogen as follows. Verschoyle[1]) investigated the vapour-liquid equilibrium of this system at temperatures 63.1, 68.1, 78.1 and 88.1°K. In almost all these isotherms the lowest pressure was about 17 atm while the highest pressure was about 225 atm. The first two isotherms form open loops while the others form closed ones in this pressure range. Verschoyle reported also some data for two isotherms below the triple point of nitrogen at 58.1 and 60.6°K. Ruhemann and Zinn[2]) made some measurements at three different temperatures, 78, 83, and 90°K. Pressures used ranged between 12 and 50 atm. The measurements of Steckel and Zinn[3]) were done at temperatures still higher than those mentioned above. Dokoupil, Van Soest and Swenker[4]) carried out measurements at temperatures between 35 and 60°K while the pressure range extended from 1.3 up to 50 atm. The equilibrium studied in this work is mainly the equilibrium between gas and solid phases.

Surveying the vapour-liquid data it was found that the vapour points (dew curve), when plotted from results of Verschoyle, were rather difficult to extrapolate to lower pressures, especially for the isotherms of 63.1 and 68.1°K. The liquid points are of sufficient accuracy and one can extrapolate these boiling curves to low pressures making use of Henry's law.

In this work it was decided to perform some measurements in the vapour phase for low and moderate pressures. A graphical method is proposed to extrapolate the vapour points down to very low pressures if measurements have only been carried out at higher pressures. The thermodynamical approach correlating the vapour and liquid points is worked out for this system.

2. *Experimental procedure.* The flow method has been used in this work. A prepared mixture was allowed to stream slowly but continuously through the equilibrium vessel, the latter being kept at a chosen fixed temperature and pressure. The vessel was surrounded by a cryostat filled with liquid oxygen boiling under adjusted pressure. The temperature was controlled by means of regulating the pressure in the dewar vessel. In this way we could keep the temperature constant within 0.1°K. Stirring of the bath proved to be necessary, especially when working with oxygen as refrigerant. This was done by means of small rotating propellers driven by an electric motor placed outside the cryostat.

The temperature was determined with a platinum thermometer calibrated against a standard one. The pressure was read on a Bourdon manometer with accuracy of ± 0.1 atm. Before sampling the apparatus was allowed to run for 20 minutes which proved to be sufficient time for attaining a stationary state and thus equilibrium; then sampling of the gas phase took place slowly in an evacuated glass balloon. During one run it was possible to obtain three different samples for three different pressures at a single temperature.

The analysis apparatus which was originally constructed for determination of very small amounts of nitrogen in H_2–N_2 mixtures limited our work to concentrations up to 12%. The analyzing procedure and apparatus are described in details in ref. [4]). In principle it consists in circulating a given quantity of the sample through the analysis circuit part of which is a glass capillary immersed in liquid hydrogen. The nitrogen content will freeze out with negligible vapour pressure. The gaseous hydrogen left is then pumped off completely. The solidified nitrogen can then be warmed up and is allowed to expand into the system. From the known initial filling pressure of the sample, the partial pressure of the separated nitrogen and from knowing the volumes of the analysis system the nitrogen concentration in the sample can then be calculated.

Above 63.15°K nitrogen becomes liquid and from the results of Verschoyle we knew that the solubility of the volatile component (hydrogen) in the liquid is no longer negligible as it was in the case of solid-gas equilibrium below 63°K. In this case, however, determination of the liquid-phase sample would have required another analyzing method adopted for detection of small quantities of hydrogen in liquid nitrogen. As it has been mentioned before that seemed unnecessary since we can easily extrapolate the liquid points to lower pressures using Henry's law with reasonable accuracy.

3. *Results.* Both gases hydrogen and nitrogen were obtained from laboratory stock. Hydrogen of purity 99.9% was passed through a silica gel kept at nitrogen temperature in order to remove all usual impurities. The purity of nitrogen was about 99.8%, this was already sufficient for our purpose and therefore no further purification was done.

Table I contains the partial pressures of nitrogen in hydrogen and the molar concentration x_1, of nitrogen in the vapour in equilibrium with the liquid phase at 5, 10, 15, 25, 35 and 45 atm respectively.

TABLE I

5 atm			10 atm			15 atm		
T °K	p_1 atm	x_1	T °K	p_1 atm	x_1	T °K	p_1 atm	x_1
63.6	0.169	0.0338	63.6	0.213	0.0213	63.7	0.274	0.0183
68.0	0.338	0.0676	68.1	0.475	0.475	68.1	0.579	0.0386
72.2	0.580	0.116	72.3	0.752	0.0752	72.4	0.907	0.0605
74.6	0.620	0.124	74.7	1.03	0.103	74.7	1.18	0.0787
25 atm			35 atm			45 atm		
T °K	p_1 atm	x_1	T °K	p_1 atm	x_1	T °K	p_1 atm	x_1
63.1	0.327	0.0131	63.15	0.437	0.0125	63.0	0.625	0.0139
68.1	0.687	0.0275	68.25	0.934	0.0267	68.05	1.24	0.0276
72.5	1.15	0.0462	72.5	1.50	0.0429	72.5	1.97	0.0437
74.9	1.28	0.0515	75.2	1.87	0.0535	75.0	2.40	0.0533

The temperatures were chosen at 63.1 and 68.1°K to redetermine the lower parts of the isotherms measured by Verschoyle 1). Another two isotherms at 72.3 and 74.6°K were measured to cover the intermediate region.

Fig. 1 gives our results in a T-x diagram. Some points of measurements of Dokoupil, Van Soest and Swenker 4) are included for comparison and show the continuity of the equilibrium curves when nitrogen changes phase at the triple point. There is no observable change of the slope at this temperature.

The gaseous branch of the equilibrium loops in the p–x diagram is given in fig. 2 at constant temperature. The points measured by Verschoyle are included in order to show both pressure regions of interest.

The partial pressure of nitrogen p_1 in hydrogen is plotted in fig. 3 as a function of the reciprocal temperature and compared with the vapour pressure of liquid nitrogen.

Such a plot is convenient for the purpose of smoothing the results.

The enhancement factor is given by the ratio of the partial pressure px_1

of nitrogen in hydrogen and the vapour pressure p_{01} of pure nitrogen $f = px_1/p_{01}$. This factor f has been calculated from our results and is shown in fig. 4 as a function of pressure for different isotherms. The enhancement factor f is larger than 1; in this mixture the interaction between unlike molecules makes the partial pressure larger than in the case of validity of Dalton's law. From the plots of points in table I it follows that the accuracy is about 2%.

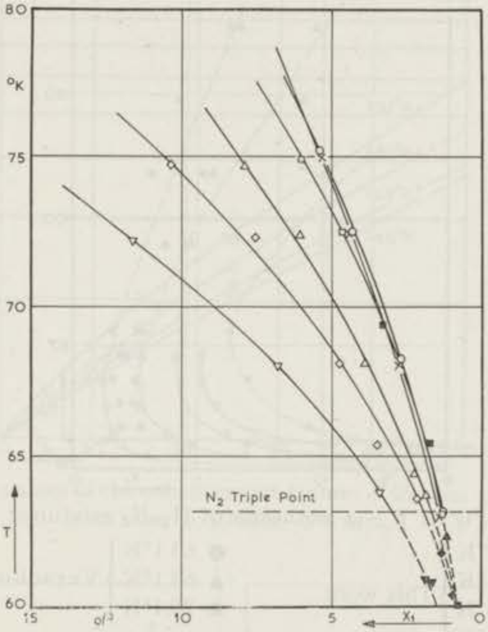

Fig. 1. $T - x$ isobars of H_2–N_2 mixtures:

▽ 5 atm, □ 25 atm }
◇ 10 atm, ○ 35 atm } This work
△ 15 atm, × 45 atm }

▼ 5 atm }
◆ 10 atm }
▲ 15 atm } Dokoupil *e.a.*[4])
■ 25 atm }

Fig. 5*a* represents the complete p–x equilibrium loop which qualitatively applies to our system under consideration: the boiling curve, p^L, rises from the nitrogen axis up to the plait point C; the dew curve p^G begins from the same starting point on the nitrogen axis, passes through the critical point of contact C' and subsequently merges into p^L at C. The coexisting points of both phases are characterized by a horizontal connodal line. When the loop is known in the whole extent both partial pressure curves p_1 and p_2 can be calculated and have the indicated qualitative positions.

Fig. 5*b* illustrates a familiar p–x diagram for a L + G equilibrium when critical points of components are not far apart. The partial pressure curves p_1 and p_2 usually follow the laws of Raoult and Henry in limited concentration ranges. Such properties of the equilibrium curves simplify the possible extrapolation of measured points in the neighbourhood of the ends of the equilibrium loops.

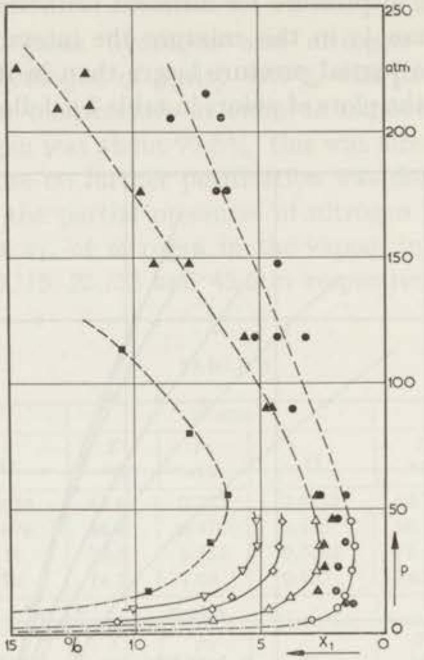

Fig. 2. $p - x$ isotherms of H_2–N_2 mixtures:

○ 63.1°K
△ 68.1°K
◇ 72.3°K
▽ 74.6°K
} This work

● 63.1°K
▲ 68.1°K
■ 78.1°K
} Verschoyle [1])

–·–·–·–· low pressure values extrapolated by the graphical method.

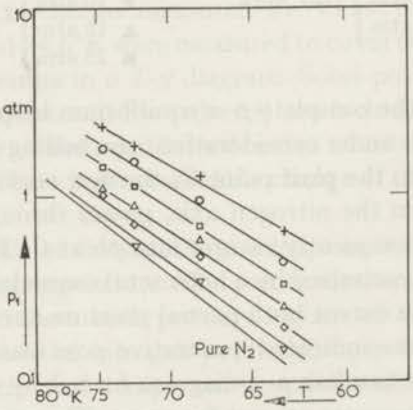

Fig. 3. Partial pressures of N_2 in H_2 as a function of temperature at constant pressures: + 45 atm, ○ 35 atm, □ 25 atm, △ 15 atm, ◇ 10 atm, ▽ 5 atm and vapour pressure of nitrogen.

For the isotherms of nitrogen-hydrogen mixtures p^L is known well enough from the measurements of Verschoyle [1]). His dew points cover the high pressure region between *C* and *C'* (see fig. 5*a*), and our measurements define accurately the region of the bend of the dew curve below the critical point of contact *C'* down to 5 atm.

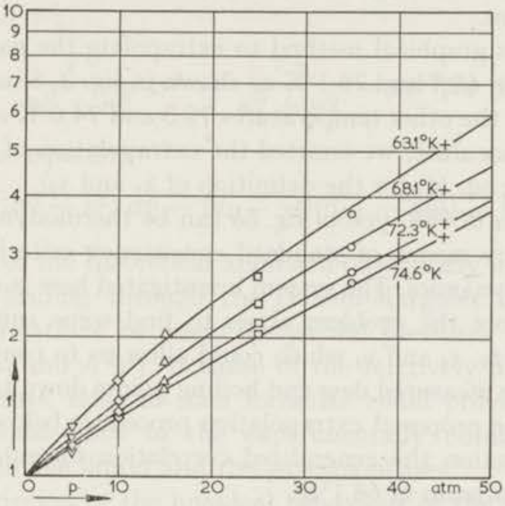

Fig. 4. Experimental values of the enhancement factor: + 45 atm, ○ 35 atm, □ 25 atm, △ 15 atm, ◇ 10 atm, ▽ 5 atm.

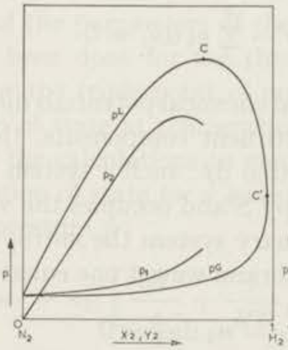

Fig. 5*a*. $p - x$ isotherm for a mixture with components differing much in critical points.

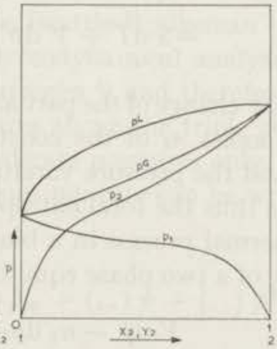

Fig. 5*b*. $p - x$ isotherm for a mixture when critical points of components are not far apart.

The rest of the curve is to be determined by extrapolation.

Although there is an essential dissimilarity between the diagrams presented in fig. 5*a* and 5*b*, a similar extrapolation applicable to the curves of fig. 5*b* is proposed to be applied for the equilibrium curves of fig. 5*a* as well. From the measured concentrations x_1 down to 5 atm $p_1 = px_1$ is calculated and $p_2 = p - p_1$ plotted for the same pressure interval as a function of the corresponding concentration. p_2 proves to be linear in the region of moderate pressures and, therefore, it seems to be justifiable to extrapolate p_2 linearly down to zero pressure. The same applies to the extrapolation of p. So we get p_1 and hence x_1-values in the low pressure region below 5 atm.

We applied this graphical method to extrapolate the gaseous curves for the isotherms 63.1, 68.1 and 78.1°K as shown in fig. 2. Since no liquid data were available for the other temperatures 72.3 and 74.6°K and interpolation of y_2 is rather inaccurate, we omitted the extrapolation of x_1 for these two temperatures (see eq. (4) for the definition of x_i and y_i).

Phase equilibria of the type of fig. 5*b* can be thermodynamically treated at low pressures by means of standard consistency criteria given in textbooks of thermodynamics. The system investigated here is of the type given in fig. 5*a*; therefore the problem arises to find some suitable correlation formula between p_i, x_i and y_i which could allow us to control not only the consistency of the measured dew and boiling points down to 5 atm, but also the validity of the proposed extrapolation procedure below 5 atm.

In the next section the generalized correlation formula is derived and applied for the isotherm of 68.1°K.

4. *Thermodynamical analysis*. The general Gibbs-Duhem relation written in the usual differential form

$$-S\,\mathrm{d}T + V\,\mathrm{d}p - \sum_{i=1}^{k} n_i\,\mathrm{d}\mu_i = 0 \qquad (1)$$

expresses how the change of the partial chemical potentials $\mathrm{d}\mu_i$ depends upon the number of moles n_i of the constituent components, the temperature variation $\mathrm{d}T$ and the pressure variation $\mathrm{d}p$; such a system consisting of a single phase has thus the total entropy S and occupies the volume V.

For an isothermal process in a binary system the entropy term $S\,\mathrm{d}T$ is zero and in case of a two phase equilibrium we get one equation of type

$$V\,\mathrm{d}p - n_1\,\mathrm{d}\mu_1 - n_2\,\mathrm{d}\mu_2 = 0 \qquad (2)$$

for each phase. Let us denote each of the phases by the superscripts G and L for gaseous and liquid phases respectively; the subscript 1 refers to nitrogen and 2 to hydrogen. When subtracting the resulting two equations having the form (2) from each other and using the equilibrium equality of the μ's in both phases we get

$$(V^{\mathrm{G}} - V^{\mathrm{L}})\,\mathrm{d}p - (n_1^{\mathrm{G}} - n_1^{\mathrm{L}})\,\mathrm{d}\mu_1 - (n_2^{\mathrm{G}} - n_2^{\mathrm{L}})\,\mathrm{d}\mu_2 = 0. \qquad (3)$$

The substitution of x_i for the mole fraction of the gaseous phase and y_i for the mole fraction in the liquid phase,

$$x_i = \frac{n_i^{\mathrm{G}}}{n_1^{\mathrm{G}} + n_2^{\mathrm{G}}}, \; y_i = \frac{n_i^{\mathrm{L}}}{n_1^{\mathrm{L}} + n_2^{\mathrm{L}}} \qquad (i = 1, 2), \tag{4}$$

the definition of the molar volume in the gaseous phase v^{G} and the expression for the molar volume v^{L} in the liquid phase by means of the partial molar volumes V_1^{L} and V_2^{L},

$$v^{\mathrm{G}} = \frac{V^{\mathrm{G}}}{n_1^{\mathrm{G}} + n_2^{\mathrm{G}}}, \; v^{\mathrm{L}} = \frac{V^{\mathrm{L}}}{n_1^{\mathrm{L}} + n_2^{\mathrm{L}}} = y_1 V_1^{\mathrm{L}} + y_2 V_2^{\mathrm{L}} \tag{5}$$

yields finally the equation

$$(v^{\mathrm{G}} - v^{\mathrm{L}})\, \mathrm{d}p - (x_1 - y_1)(\mathrm{d}\mu_1 - d\mu_2) = 0. \text{ 5)} \tag{6}$$

At this stage of the theoretical approach one usually introduces standard simplifications leading through the Duhem-Margules relation to various differential correlations between the partial pressures $p_i = px_i$ and the mole fractions x_i and y_i 5)6)). Because of the relatively high pressures used in our experiments, none of such formulae could provide any means for checking the consistency of the experimentally obtained data for the concentrations in the liquid and the gaseous phases.

For the description of the nonideal behaviour of the gaseous phase we must use some equation of state for a gaseous mixture; such a corresponding expression for V^{G} is further used for the calculation of the partial chemical potentials μ_i in the gaseous phase as a function of p, T and x_i. The numerical adjustments of the parameters of the Beattie-Bridgeman equation of state have already been done for the thermodynamical analysis of the system $\mathrm{H_2 + N_2}$ below the triple point of nitrogen 4) and therefore we applied the same equation of state at temperatures above the triple point of nitrogen. We restricted the calculations to moderate pressures only.

Every equation of state for a gaseous mixture can be written as a power series in the pressure p:

$$V^{\mathrm{G}} = (n_1 + n_2)\left[\frac{RT}{p} + \frac{1}{RT}\beta_m + (\ldots)\, p + (\ldots)\, p^2 + \ldots\right]. \tag{7}$$

Since we shall restrict the calculations up to the second virial coefficient β_m of the mixture we rewrite the above equation in the form

$$\begin{aligned} V^{\mathrm{G}} &= (n_1 + n_2)\left[\frac{RT}{p} + \frac{1}{RT}(x_1^2\beta_{11} + x_2^2\beta_{22} + 2x_1x_2\beta_{12})\right] \\ &= (n_1 + n_2)\left[\frac{RT}{p} + \frac{1}{RT}(x_1\beta_{11} + x_2\beta_{22} + x_1x_2D_{12})\right] \end{aligned} \tag{8}$$

where the D_{12}-coefficient is defined by $D_{12} = 2\beta_{12} - \beta_{11} - \beta_{22}$; β_{11}, β_{22} and

β_{12} are the second virial coefficients described by the Beattie-Bridgeman formalism [7][8])

$$\beta_{ij} = RTB_{ij} - A_{ij} - \frac{Rc_{ij}}{T^2} \qquad (i, j = 1, 2). \tag{9}$$

B_{ii}, A_{ii} and c_{ii} are the parameters for both pure components, B_{12} is obtained by means of the assumed validity of the Lorentz combination rule and A_{12}, c_{12} by means of the square-root combination rule of the parameters for pure components:

$$\begin{gathered} B_{12} = \tfrac{1}{8}(B_{11}^{\frac{1}{3}} + B_{22}^{\frac{1}{3}})^3 \\ A_{12} = A_{11}^{\frac{1}{2}}\, A_{22}^{\frac{1}{2}};\ c_{12} = c_{11}^{\frac{1}{2}}\, c_{22}^{\frac{1}{2}}. \end{gathered} \tag{10}$$

The equation (8) for V^{G} is used in the same approximation for the calculation of the partial chemical potentials by means of the formula [8])

$$\begin{aligned} \mu_i(p, T, x_i) &= \text{const.} + RT \ln px_i + \int_0^p \left[\left(\frac{\partial V}{\partial n_i}\right)_{p,T} - \frac{RT}{p}\right] \mathrm{d}p \\ &= \text{const.} + RT \ln px_i + \beta_{ii}p/RT + D_{ij}\,p(1 - x_i)^2/RT. \end{aligned} \tag{11}$$

The substitution of equations (8), (5) and (11) into (6) gives after the rearrangement of the different terms:

$$\frac{\mathrm{d}p}{\mathrm{d}x_1} = \frac{1}{1 + \varepsilon}\,\frac{x_1 - y_1}{x_1(1 - x_1)}\,p \tag{12}$$

while

$$\varepsilon = \frac{\left(\dfrac{p}{RT}\right)\left\{y_1\left(\dfrac{\beta_{11}}{RT} - V_1^{\mathrm{L}}\right) + (1 - y_1)\left(\dfrac{\beta_{22}}{RT} - V_2^{\mathrm{L}}\right) + \dfrac{D_{12}}{RT}\left[(1 - y_1)\, x_1^2 + y_1\,(1 - x_1)^2 + 2x_1(1 - x_1)\right]\right\}}{1 - \left(\dfrac{p}{RT}\right)\dfrac{D_{12}}{RT}\,2x_1(1 - x_1)}. \tag{13}$$

Although formula (12) is basically known we presented the complete derivation in full details in order to show explicitly at which points the difficulties arise if one tries to correlate the liquid-gas equilibrium at high pressures when the critical points of the constituent components are far apart. Such an application of (12) has not yet been done before. Any further generalization of this formula would be possible using the same way of derivation mentioned above with the equation of state including higher virial coefficients.

In the case of ideal behaviour of the gaseous phase the quantity ε becomes zero supposing that we can neglect the partial molar volumes in the liquid phase. The formula (12) is thus reduced to the known relation usually used for the correlation of one phase curve if the other equilibrium curve is available.

When there are known experimental data of high accuracy for the dew and boiling curves one can calculate from equations (12) and (13) the second virial coefficient for the mixture at low pressures as was shown by Scatchard for some hydrocarbons [9]); he used, however, another equation of state. The value of ε is small with respect to 1.

We evaluated the formulae (12) and (13) for the isotherm of 68.1°K, using the data of Verschoyle for the liquid phase and our measured and interpolated data for the gaseous phase in the pressure range from 1 up to 70 atm. The parameters of the equation of state have been taken from the above mentioned article [4]). As there are no data available for the partial molar volumes in the liquid phase we took the molar volumes of liquid nitrogen for V_1^L and we neglected V_2^L with respect to the small second term which is multiplied by a small numerical factor $(1 - y_1)$.

TABLE II

p atm	x_1	y_1	ε	$1 + \varepsilon$	$(\mathrm{d}p/\mathrm{d}x_1)_{\mathrm{calc}}$	$(\mathrm{d}p/\mathrm{d}x_1)_{\mathrm{exp}}$
1	0.30	0.998	-0.033_7	0.966	-3.44	-3.5
2	0.17	0.997	-0.062_9	0.937	-12.5	-13
3	0.1	0.995	-0.091_9	0.908	-32.9	-33
5	0.069	0.9915	-0.152	0.848	-84.6	-88
10	0.0465	0.9825	-0.304	0.696	-303	-310
15	0.038	0.974	-0.455	0.545	-705	-700
25	0.0275	0.956	-0.759	0.241	-3600	-3300
35	0.0265	0.938	-1.053	-0.053	$+23000$	$+25000$
45	0.028	0.922	-1.366	-0.366	$+4040$	$+4000$
70	0.036	0.883	-2.26	-1.26	$+1350$	$+2200$

From the results summarized in table II we see immediately that the quantity ε is no longer a correction term in the case of moderate total pressures. On the contrary it contributes essentially to the numerical value of the slope $(\mathrm{d}p/\mathrm{d}x_1)_{\mathrm{calc}}$ given in the same table in comparison with the experimental value $(\mathrm{d}p/\mathrm{d}x_1)_{\mathrm{exp}}$. The agreement between theory and experiment is quite good although the accuracy of the determination of the steep slope is decreased near the critical point of contact. The quantity $(1 + \varepsilon)$, however, passes through zero at the critical point of contact where the sign of the slope reverses. The plot of p against $(1 + \varepsilon)$ makes it possible to determine the critical point of contact accurately; this one is in good agreement with observed location of C'.

The numerical agreement of the calculated slopes and the experimental ones proves that the measured and extrapolated values of x_1 and y_1 for the pressures below 45 atm are not in contradiction with the thermodynamical requirements.

For the pressures above 45 atm the discrepancy between the theoretical slope and the experimental one becomes significant. The Beattie-Bridgeman equation of state simplified to the second virial coefficient breaks down at about 75 atm for the temperature 68.1°K; therefore we cannot expect any valid correlation in the region of high pressures, especially between the critical point of contact and the plait point of the equilibrium curve. The higher density of the gaseous phase in the region of the retrograde increase of the nitrogen concentration with pressure would require an equation of state describing adequately the behaviour of such a system up to the critical pressure. In this region the partial molar volumes in the liquid cannot be treated in the way we explained in the preceding paragraphes. Due to the lack of such data and because of the inaccuracy of the available high pressure concentration data it did not seem justifiable to us to extend the thermodynamical analysis up to the critical region using more elaborate virial expressions.

REFERENCES

1) Verschoyle, T. T. H., Trans. roy. Soc. London **A230** (1931) 189.
2) Ruhemann, M. and Zinn, N., Phys. Z. U.S.S.R. **12** (1937) 389.
3) Steckel, F. and Zinn, N., Zhurn. khim. Prom. **16**, (1939) 24.
4) Dokoupil, Z., Van Soest, G. and Swenker, M. D. P., Commun. Kamerlingh Onnes Lab., Leiden No. 297; Appl. sci. Res. **A5** (1955) 182.
5) Ruhemann, M., The separation of gases (Oxford University Press, 1949).
6) Hála, E., Pick, J., Fried, V. and Vilím, O., Vapour-liquid equilibrium (Pergamon Press 1958).
7) Beattie, J. A. and Bridgeman, O. C., Proc. amer. Acad. Arts Sci. **63** (1928) 229.
8) Beattie, J. A., Chem. Rev. **44** (1949) 141.
9) Scatchard, G. and Raymond, G. L., J. amer. chem. Soc. **60** (1938) 1278.

CHAPTER II

DETERMINATION OF THE SOLID-LIQUID EQUILIBRIUM DIAGRAM FOR THE NITROGEN-METHANE SYSTEM

Synopsis

The equilibrium between the solid and liquid phases of the nitrogen-methane system has been studied. The liquidus and solidus curves together with the three phase line of the system are determined using a combined method comprising measurements of the total vapour pressure, the heat capacity and thermal analysis of mixtures of various concentrations. Methane and nitrogen are found to be partially miscible in the solid state, the melting diagram is of an eutectic type. The eutectic concentration is 23.8% methane. Liquid nitrogen containing methane up to the eutectic concentration solidifies and melts nearly at the same temperature of 62.6°K. The liquidus and solidus curves are very close to each other in this concentration range where the temperature difference does not exceed 0.5°K. The total amount of nitrogen which is soluble in the methane lattice is less than 45%. A three dimensional space model of the phase-equilibrium diagrams of this system is constructed, and the discussion of previous work and the various experimental methods is presented. The ideal solution theory does not adequately describe the melting diagram. A better agreement with the results is obtained by considering the behaviour of the system as a regular liquid solution in equilibrium with a regular solid solution.

1. *Introduction.* At room temperature the solid-liquid equilibrium of many systems has been investigated. Only a small number of binary systems of condensed rare gases has been investigated at low temperatures below the triple point of one of the constituent components. The experimental techniques used at high temperatures can be adapted with some change for the low temperature work. The theories of solid and liquid solutions, applied with success at moderate or high temperatures, can also be used at low temperature for simple spherical molecules such as Ne, Ar, Kr, Xe, or CH_4, or for the simple spherical molecules in combination with non-spherical molecules such as N_2, CO or O_2.

The list of the measured binary melting diagrams of the above mentioned gases reveal not only the scarcity of good available data but in many cases one finds some severe discrepancies when the same system is examined in different laboratories. For instance, the purity of the pure components used for the measurements was sometimes of great importance in the earlier experiments; in other cases the single chosen experimental method could not provide good results in the whole concentration range for the corresponding temperatures and often difficulties arose from very long times needed for the attainment of thermodynamic equilibrium.

It is not the purpose of this article to give a complete discussion of existing experimental and theoretical work referring to solid-liquid equilibria at low temperatures because we are mainly interested in the behaviour of the binary system N_2–CH_4. This system was measured by M. Fedorova[1]) in 1939 and by V. G. Fastovskij and Y. A. Krestinskij[2]) in 1941. The experimental points of Fedorova obtained by the heat capacity method were in disagreement with the part of the liquidus curve reported by Fastovskij and Krestinskij. The latter investigators used the vapour pressure method together with visual observations, and their results comprised only 5 points. The heat capacity analysis of Fedorova suggested the possibility of the formation of an intermediate condensed phase which was not found by other measurements. In order to resolve the discrepancies concerning this system we decided to redetermine the complete melting diagram of N_2–CH_4. The knowledge of the freezing and melting curves of N_2–CH_4 is of importance to help the engineer when considering the blocking of heat exchangers in gas separation plants when coke-oven gas is cooled to prepare pure hydrogen for the production of synthetic ammonia.

In the following section we describe the three dimensional phase model for the N_2–CH_4 system where the three phase line and the projection of the three dimensional liquidus and solidus lines are drawn to point out our field of interest. The third section contains the description of the experimental methods. The apparatus and the measuring procedure is given in the fourth section. The fifth section presents the results, and the last section deals with the thermodynamic discussion.

2. *The three dimensional model of the N_2–CH_4 system.* Following the classical ideas of Roozeboom[3]) it is useful to present the phase equilibrium properties of a binary system by means of a three dimensional model. Especially in a pressure-temperature region where a new phase appears even a qualitative sketch can help us to understand the behaviour of the mixture. The location of the equilibrium surfaces indicates in some cases the preferable application of a specific experimental method. As we are interested mainly in the melting diagram of the nitrogen-methane mixtures we tried to develop the three-phase model for the temperature interval between the triple points of both pure components and for the adjoining higher temperatures. We omitted, therefore, the critical region and the part at lower temperatures where a solid solution is in equilibrium with a gaseous phase only. We investigated the above mentioned mixture under the satu-

ration pressure, in most cases, and the pressure interval of the space model restricted to low pressures only: from the triple point pressures of both pure components to about 2.5 atm.

The basic elements needed for the construction of a three-phase model in the mentioned $p - T$ extension are the $T - x$ diagrams for the gas-liquid equilibrium (G + L) at constant pressure p, and the isobaric liquid-solid diagrams (L + S). An illustration of such diagrams is given in fig. 1 for three different pressures of about 2, 0.7 and 0.25 atm. The G + L equilibrium loops are extrapolated from the work of Bloomer and Parent[4]). The qualitative L + S loops taken from the preliminary measurements of Fedorova[1]) and of Fastovskij and Krestinskij[2]) show a kind of a degenerate eutectic equilibrium with a very narrow loop near the nitrogen axis, drawn here as a single straight line for simplicity. With decreasing pressure both phase complexes sketched in fig. 1*a* (2 atm) are coming close together, they touch each other in fig. 1*b* (0.7 atm) and interprenetrate finally as indicated in fig. 1*c* (0.25 atm.) The location of the L + S complex is rather pressure independent in the low pressure region.

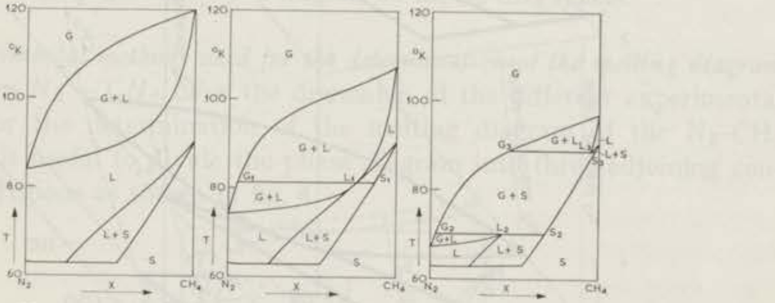

Fig. 1*a*, 1*b*, 1*c* $T - x$ isobars of the N_2–CH_4 system at 2 atm, 0.7 atm and 0.25 atm respectively.

In fig. 2 the $T - x$ diagrams, which constitute the isobaric sections of the three dimensional model, show that the G + L equilibrium surfaces contact each other along the vapour pressure curves of the constituent pure components. The L + S equilibrium surfaces contact each other along the melting curves and the G + S equilibrium surfaces along the sublimation curves. On the $p - T$ side planes one recognizes easily the characteristic $p - T$ plot for the pure components in the neighbourhood of the triple points T_{CH_4} and T_{N_2} respectively.

The isobaric planes *A*, *B*, *C* refer to the three diagrams in fig. 1.

The space enclosed between any two corresponding equilibrium surfaces forms an inhomogeneous region. Any two coexisting states in phase equilibrium are indicated by a connodal line which is thus parallel to the concentration axis. The merging of the G + L lens into the L + S loop gives rise to a three-phase equilibrium G + L + S. The corresponding connodals

$G_i - L_i - S_i$ $(i = 1, 2, 3)$ (see fig. 2) describe the solidification of the liquid mixture under its own vapour pressure. Such an equilibrium is univariant according to the Gibbs phase rule. The locus of the points L_i constitutes the three dimensional three-phase line $T_{CH_4} - L_3 - L_1 - L_2 - E$ in fig. 2. The same name is often used for the corresponding orthogonal projection on the $p - T$ plane $T_{CH_4} - L'_3 - L'_2 - L'_1 - E'$; these points, of course, coincide with the points $T_{CH_4} - S'_3 - S'_1 - c'_2 - D'$ given in fig. 3. This three-phase line starts at the triple point of methane and would end in the quadruple point of the system.

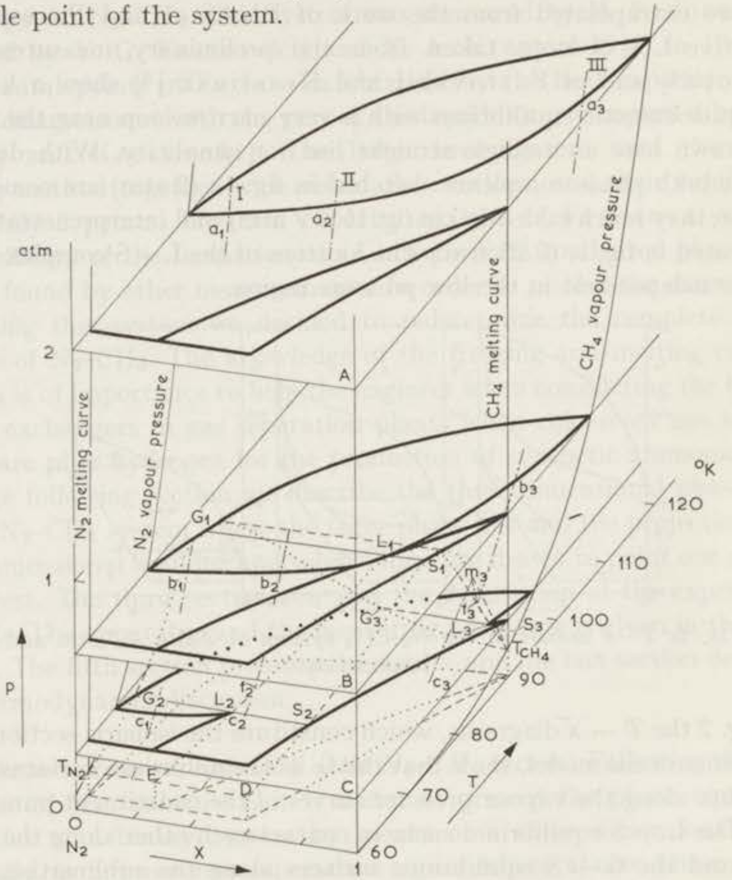
III
a3
II
I
a1
a2
atm
2
A
N2 melting curve
N2 vapour pressure
CH4 melting curve
CH4 vapour pressure
°K
120
110
100
90
80
70
60
b3
G1
L1
S1
m3
b1
b2
1
G3
f3
L3
S3
TCH4
p
B
c3
f2
G2
L2
S2
c1
c2
TN2
E
D
C
T
O
O
N2
X
1
CH4

Fig. 2. Three dimensional model for the system N_2–CH_4.

Strictly speaking the solidus line and the parts of the liquidus line belonging to the two phase equilibrium L + S (or G + S) should be measured isobarically (see figs 1*a*, 1*b*, 1*c*).

As both phase lines are practically pressure independent, one usually performs the measurements under the variable saturation vapour pressure. In a single $T - x$ plot (see fig. 15) one collects all points L_i for the freezing line and all S_i points for the melting line. Such an orthogonal projection of the liquidus and the solidus lines on the $T - x$ plane is represented by broken lines in fig. 2.

Using different experimental methods we determined the above mentioned melting diagram, and the corresponding three-phase line of the nitrogen-methane system.

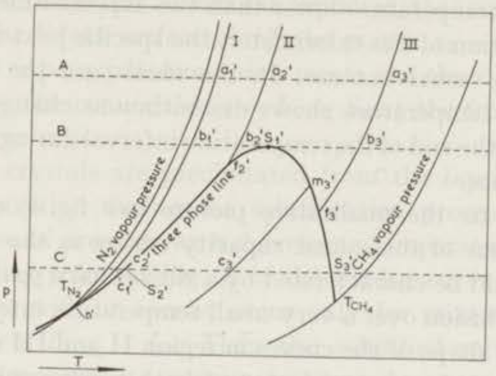
I
II
III
A
B
C
a_1'
a_2'
a_3'
b_1'
b_2'
S_1'
b_3'
f_2'
m_3'
f_3'
c_2
c_3
c_1'
S_2'
S_3'
T_{N_2}
T_{CH_4}
N_2 vapour pressure
three phase line
CH_4 vapour pressure
p
T

Fig. 3. Qualitative p–T diagram for the N_2–CH_4 system.

3. *Experimental methods used for the determination of the melting diagram of the system* $N_2 - CH_4$. For the discussion of the different experimental methods for the determination of the melting diagram of the N_2–CH_4 system, it is useful to divide the phase diagram into three adjoining concentration regions as shown in fig. 4.

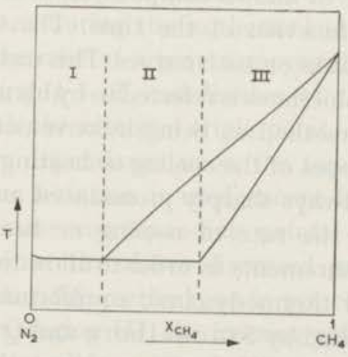
I
II
III
T
O
N_2
x_{CH_4}
1
CH_4

Fig. 4. The different concentration regions of the melting diagram.

In the region I from the nitrogen axis up to the eutectic concentration, the phase diagram is reduced to a very narrow loop as stated in the description of fig. 2.

The usual type of an eutectic loop is found in the region II between the eutectic point and the end of the solubility gap in the solid solution. Region III of the phase diagram represents the case of mixed crystals and extends up to the methane axis.

From fig. 4. combined with figs. 2 and 3 it is possible to decide which experimental method is preferable for the investigation of the melting diagram of the N_2–CH_4 system.

A. Heat capacity method. In this method the mixture of a known composition is condensed in an adiabatic calorimeter, which is cooled with its contents to a temperature lower than the expected melting point. After the thermal isolation of the calorimeter, the specific heat measurements are performed in the usual manner. In the ideal case the plot of the heat capacity against temperature shows discontinuous changes of slope at the beginning and at the end of the temperature interval during which the melting process takes place.

With respect to the qualitative picture (see fig. 4) one would expect different behaviour of these heat capacity curves in the regions I, II, III. The region I would be characterized by a single sharp peak resulting mainly from the heat of fusion over a very small temperature interval. On the other hand the general shape of the curves in region II and III is governed by the combined effect of the heat of fusion of both components and the heat of mixing in both phases.

Ruhemann$^{9)}$ and his collaborators$^{10)}$ used this method to determine the melting diagrams of the following binary systems: CH_4–C_2H_4, CO–N_2 and N_2–O_2. The measurements of Fedorova$^{1)}$ were carried out using the heat capacity method for the systems Ar–N_2, Ar—O_2, CH_4–Ar and CH_4–N_2.

B. The thermal method. The principle of this method is to cool down or to heat up a mixture of known composition in a calorimeter and to plot the temperature as a function of the time. The transition temperatures appear as pronounced kinks on such curves. This method has been developed by Tamman$^{11)}$, and sometimes is referred to by his name. Some authors$^{1)7)9)}$ described the thermal method as being inconvenient for low temperature work: the changes of slopes of the cooling or heating curves at the transition temperatures are not always sharply pronounced and they may be difficult to localize; therefore, the rate of cooling or heating must be carefully controlled in such measurements in order to allow the time sufficient for the thermal effects and for thermodynamic equilibrium.

This method was applied by Stackelberg and Quatram$^{12)}$ who studied the melting diagram of Kr–CH_4 and has shown that this system forms a complete series of mixed crystals. Veith and Schröder$^{13)}$ used the same method for four binary systems: Kr–CH_4, Ar–CH_4, Ar–Kr and Ar–O_2. The condensed phase diagram of the ternary system O_2–Ar–N_2 together with the binary mixtures of the constituent components were determined by Long and Di Paolo$^{14)}$ by means of the cooling and heating curves. Recently the Ar–Xe system was investigated by Heastie and Lefèbvre$^{15)}$ over a limited concentration range (2.7–62 mole percent Xe) using the thermal-analysis method combined with vapour pressure measurements.

C. Vapour pressure method. The principle of this method consists in following the vapour pressure while cooling down (or heating up) a condensed mixture of a known composition. The transition points will be detected as kinks on the vapour pressure curves (frequently plotted as log p against $1/T$) as it will be clear from the illustration in figs. 2 and 3. The vapour pressure of the condensed liquid in the region III follows, during cooling, the liquid surface along the points $a_3 - b_3$. At still lower temperatures the vapour pressure curve meets the three phase cylindrical surface formed by the connodals $G_i - L_i - S_i$ at the freezing point f_3 on the liquidus curve.

The first solid crystals are precipitated from the liquid solution which changes its composition during the solidification process. We observe a retrograde increase of pressure with decreasing temperature until the state given by the melting point m_3 (fig. 2) of the solidus curve is reached. Such a retrograde effect will, of course, occur only for mixtures with freezing points, f_3, between $T_{\mathrm{CH}_4} - L_1$. Then the solidified mixture regains its original composition, and its vapour pressure decreases with decreasing temperature following the points $m_3 - c_3$.

The vapour pressure of a mixture in the region II shows a similar behaviour as in the previous case: see the points $a_2 - b_2 - f_2 - c_2$ in fig. 2. There is no retrograde pressure increase because the point f_2 always lies on the low temperature side of the three-phase surface. Only the freezing point but not the melting point can be observed. The vapour pressure of a mixture in region I follows the points $a_1 b_1 c_1$ until the eutectic temperature is reached where it remains constant during the isothermal solidification of the liquid mixture analogous to the case of a pure component when passing its triple point. The corresponding $p - T$ coordinates of the points f_1, m_1 would practically coincide with the nitrogen triple point. Besides in fig. 2 the described vapour pressure dependance upon the temperature is shown once more in fig. 3. The same notation is used except for a prime representing the projection of the same corresponding points of fig. 2 on the $p - T$ plane. Taking into account the above discussed properties of the vapour pressure curves we see that this method can in principle provide the freezing and melting points in the region III, the freezing points in the region II and no accurate information at all in region I.

In order to perform the vapour pressure measurements, it is required that the liquid concentration remains unchanged during the cooling (or heating) procedure. This necessitates that the equilibrium vessel must be filled completely with the condensed liquid phase, consequently the dead volume constituting the tubing and pressure measuring device must be comparatively very small.

The vapour pressure method has been used earlier by Stackelberg, Heinrichs and Schulte[5]) for the binary systems O_2–Xe and O_2–Kr. The measured points are limited within the concentration ranges: from 10 to about 20% Xe in the system O_2–Xe, while from about 20 up to 30% Kr in the system O_2–Kr. Verschoyle[6]) determined the freezing point curve for the binary system CO–N_2 using visual observations simultaneously. The point at which the minute crystals disappeared was taken as the freezing point for the given mixture. The solid-liquid phase equilibrium diagram for the system Ar–Kr has been determined by Heastie[7]). Din, Goldman and Monroe[8]) measured the liquidus curves for the binary systems Ar–O_2 and Ar–N_2 using the same method. The data of Fastovskij[2]) for the O_2–CH_4 and N_2–CH_4 systems were obtained using the vapour-pressure method combined with direct visual observations.

In all the above mentioned investigations with the exception of the Ar–Kr system measured by Heastie, the vapour-pressure method provided data only for the freezing-point curve. The Ar–Kr system forms a complete series of solid solutions.

4. *Apparatus and experimental procedure.* The general scheme of the apparatus is given in fig. 5. The cylinders *A* and *B* contained pure gaseous methane and nitrogen respectively. The pressure in either cylinder could be given by the manometer M_1. The tap V_1 allowed the constituent gases to be mixed in the mixture cylinder *C* which had a volume of about 5 liters.

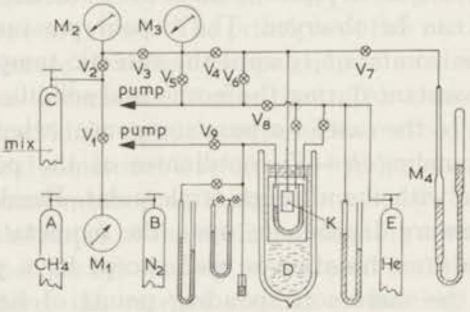

Fig. 5. The apparatus.

The component whose concentration would be less than 50% in the mixture, was first admitted into *C* and its partial pressure was read on a calibrated Bourdon manometer M_2. The pressure range of M_2 was 0–15 atm with a scale of 300 divisions; the accuracy of pressure measurements using this manometer was 0.015 atm. In cases when the pressure was less than 1 atm the mercury manometer M_4 was switched in the mixing circuit through the taps V_3, V_4 and V_7. The total pressure indicated the final pressure of the mixture after introducing the second component into *C* and concentration was evaluated from the recorded pressures. The inaccuracy in determining the concentrations is estimated to be less than 0.5%. The freshly prepared mixture was usually allowed to stand over at least one night before use to insure complete mixing.

In this work two all-metal calorimeters were subsequently used. The calorimeter shown in fig. 6*b* was mostly used for pressures under 1 atm while the other calorimeter shown in fig. 6*a* could be used for high pressure measurements. The same notation is chosen to refer to the identical parts in both calorimeters. The calorimeter vessel K had a volume of 14.1 cm^3 for apparatus (*a*) and 5.9 cm^3 for apparatus (*b*). Both vessels were made from copper with wall thicknesses of 2 and 0.5 mm respectively. The stirrer S was thick copper wire (2 mm diameter) wound in a helical form and was attached to a piece of soft iron by means of a thin stainless steel wire passing through the filling capillary C_3. The iron piece was enclosed inside a vacuum-tight glass housing placed outside the cryostat. A small magnet activated that stirrer device and the resulting up and down movement of S provided reasonable temperature equilibration in the condensed mixture. The stirring was possible, of course, in the liquid phase only.

The platinum thermometer R was placed in a hole, constructed axially in the calorimeter vessel K, and was surrounded with Woods metal to insure good thermal contact. We used the platinum resistance thermometers of the glass enclosed type manufactured by Degussa (Degussa, Hanau, West Germany). The ice point of both thermometers was about 100 ohm, and both were calibrated against a standard thermometer for the temperature region 55–90°K. The accuracy in the temperature measurements was about 0.05°K.

Heating of the calorimeter vessel was done electrically by means of a heater H_1 wound noninductively around K. The heater was surrounded by an aluminum foil to reduce radiation effects and to protect the heater. In order to prevent blocking of the filling capillary C_3 a large heater H_2 was put around it. In the second apparatus (*b*) an extra heater H_3 was used to keep the temperature of the shield close to that of the calorimeter. The electrical leads of the heaters and the thermometer were connected to the outside of the calorimeter assembly by means of platinum-glass seals W_1 and W_2.

E_1 and E_2 represent the internal vacuum insulation spaces around the calorimeter vessel K, and the external one in contact with the main bath D. These spaces were filled with He exchange gas under a pressure of few centimeters mercury. The whole assembly was first cooled to a temperature near that of the main bath D and subsequently the calorimeter K was cooled by means of the small inner bath B, where liquid nitrogen (or liquid oxygen) was used as refrigerant. When the calorimeter attained a temperature of 75°K, condensation of the gas mixture from C took place in controlled steps in such a manner that the proper manipulation of the taps V_2, V_3 and V_4 together with the manometers M_2 and M_3 allowed us to follow easily the condensing process, and to notice accurately the moment when the calorimeter vessel became completely filled with the condensed mixture. The dead volume above *K*, filled with the gaseous phase, was reduced by closing V_4 and thus becomes negligible in comparison with the amount of mixture condensed in *K*. Thus it could be considered that the condensed phase had the same initial composition as that in *C*.

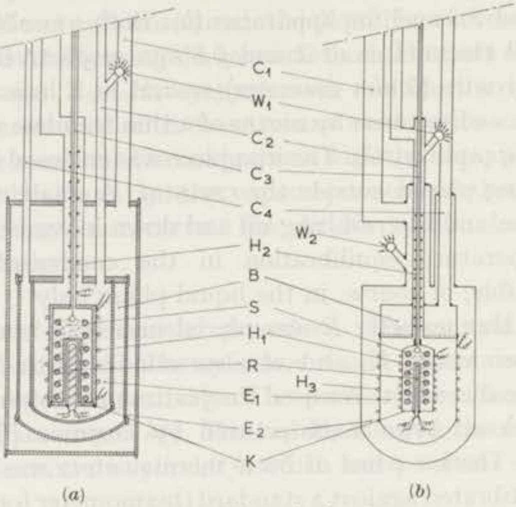

Fig. 6*a*, 6*b*. The calorimeters.

When the mixture was condensed, the main bath *D* was reduced to about 68°K, the He gas in M_2 was then pumped off and further cooling of *K* was obtained by reducing the small inner bath *B*. The lowest temperature reached in this manner was about 55°K. During the cooling process the stirrer was continuously activated and both the cooling curve and the vapour pressure were simultaneously determined. After reaching a temperature sufficiently lower than the expected melting point, the helium exchange gas in M_1 was pumped off by the diffusion pump and the standard heat capacity measurements were carried out, or the continuous heating curve was determined with an adjusted heat input.

5. *Experimental results.* Nitrogen gas was supplied from the laboratory stock with a purity not less than 99.8%. Two different supplies of methane were used with a purity claimed to be 99.9% and 99.64% according to mass spectroscopic analysis.

The heat capacity curves show different character for concentrations in the different regions of the equilibrium diagram (see fig. 4). For mixtures in region I the heat capacity curve shows a single sharp peak. The ends indicate the beginning and completion of the melting process. An example of such a peak is given in fig. 7 where the heat capacity (the scale is arbitrary) is shown for a mixture with 10.0% methane.

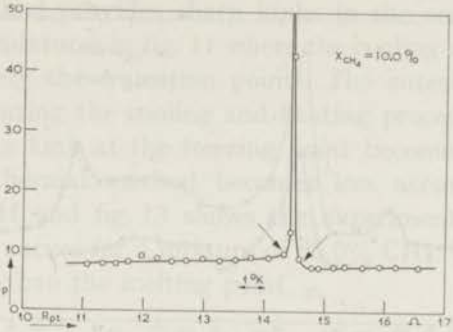

Fig. 7. Heat capacity curve for a mixture with 10.0% CH_4.

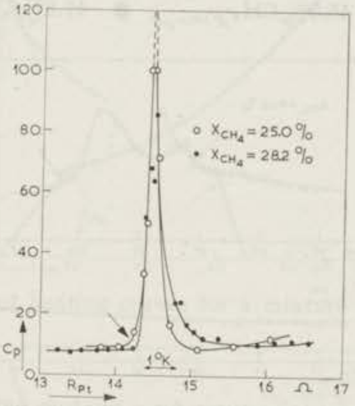

Fig. 8. Heat capacity curves for two mixtures.
○ 25.0% CH_4 ● 28.2% CH_4

In fig. 8 the corresponding curves are given for two mixtures in region II with concentrations just higher than the eutectic one. The peak is still well defined and becomes broader for mixtures higher in methane content. For still larger concentrations of methane in region II the heat capacity curves show two peaks, the first one describing the melting of the eutectic mixture and the second peak for the melting of the remaining homogeneous solid mixture. If the temperature interval between the freezing and the melting points is small, the two peaks merge together forming one peak as in fig. 8. As the methane concentration increases, the two peaks move apart and the second peak becomes less pronounced as illustrated in fig. 9 for a mixture with 45.0% CH_4. Region III shows the case of complete mixed crystals and fig. 10 shows the heat capacity measurements started at a sufficiently low temperature (about 58°K) showing the absence of any solid-solid transition in this region. The general shape of the heat capacity curve during the fusion is governed by the various processes of melting, mixing and warming up which take place simultaneously in the system. These processes are responsible for the final shape of the heat capacity curve

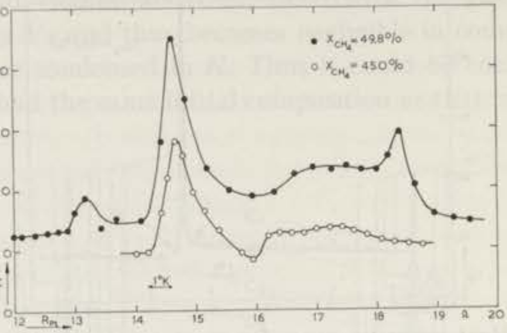

Fig. 9. Heat capacity curves.

○ 45.0% CH_4 ● 49.8% CH_4

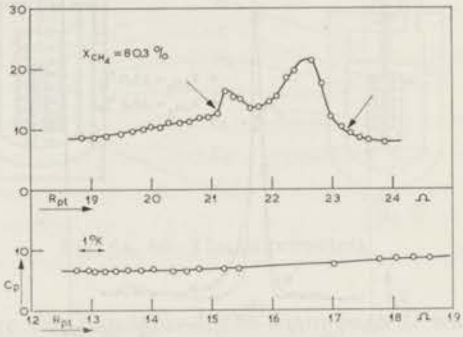

Fig. 10. Heat capacity curve for a mixture with 80.3% CH_4.
(Lower curve shows extension of measurements down to about 56°K).

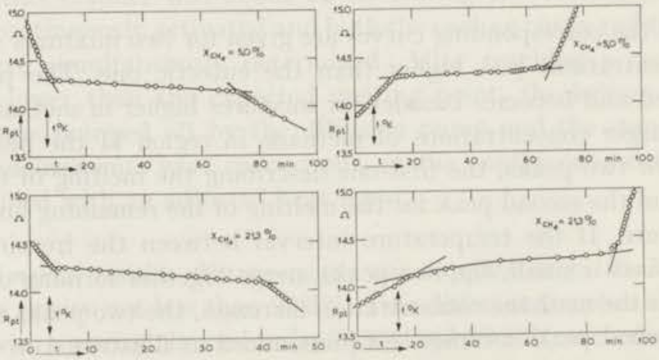

Fig. 11. Cooling and heating curves;
upper curves for 5.0% CH_4, lower curves for 21.3% CH_4.

in both regions II and III, where the temperature interval between the melting and the freezing points is relatively large. According to our experience with the heat capacity method, the melting points could be detected more accurately than the freezing points.

The thermal method provides sharp kinks in the concentration region I as shown for two mixtures in fig. 11 where the cooling and heating curves reproduced accurately the transition points. The eutectic temperature is quite pronounced during the cooling and heating procedures for mixtures in region II, but the kink at the freezing point becomes less well-defined (see fig. 12). The thermal method becomes less accurate for the concentration region III and fig. 13 shows the experimental results for the cooling and heating curves for a mixture of 85.0% CH_4. The freezing point is more pronounced than the melting point.

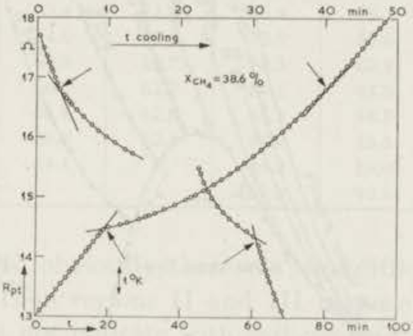

Fig. 12. Cooling and heating curves for a mixture with 38.6% CH_4.

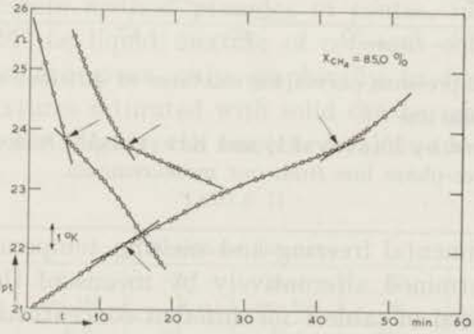

Fig. 13. Cooling and heating curves for a mixture with 85.0% CH_4.

The results obtained with the vapour pressure method for various mixtures are represented on a $p - T$ diagram shown in fig. 14, where the vapour pressure data for the pure constituent components N_2 and CH_4 are also given. The behaviour of the vapour pressure curves for mixtures in region I are nearly identical with those for pure components where the vapour pressure remains constant during the eutectic halt. For mixtures in region II, with methane content up to about 50%, the kinks on the vapour pressure curves at the freezing points are rather difficult to localize since the three-phase line lies close to the vapour pressure curves of the non-saturated liquid mixtures. The vapour pressure method allows accurate location of the freezing points in the concentration region III where the kinks at the three-phase line become more sharply defined .On the other hand, the melting points were difficult to determine. The vapour pressure of the solid solutions in region III were expected to depart from the three-phase line at the corresponding melting points (see point m_3' in fig. 3). This feature was poorly observed, and in some cases the tendency for the departure from the three-phase line was observed to lag one or two degrees below the actual melting point.

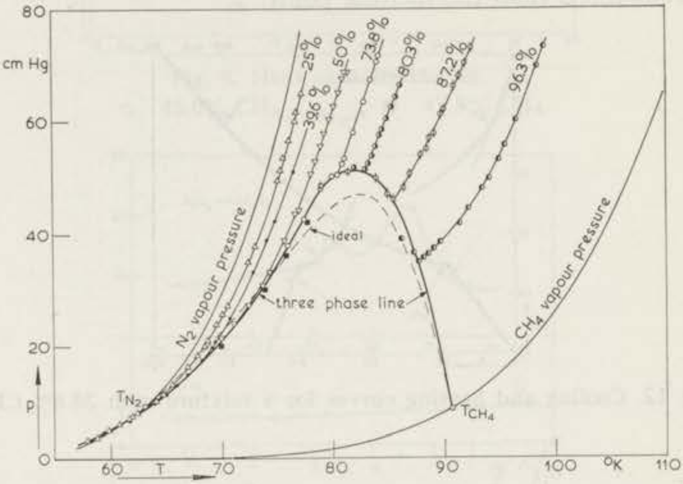

Fig. 14. Vapour pressure curves for mixtures of different methane content

---- ideal three-phase line

■ points measured by Fastovskij and Krestinskij [2]) for the three-phase line

—— smoothed three-phase line from our measurements.

Our best experimental freezing and melting temperatures (T^{f} and T^{m} respectively) determined alternatively by means of the above described procedures are listed in table I for different concentrations of the N_2–CH_4 system.

These data are plotted as a $T - x$ diagram of the system under its own vapour pressure shown in fig. 15.

The earlier measurements on this system are included in the same diagram for comparison. Our measurements show excellent agreement with the five points of the liquidus curve determined by Fastovskij and Krestinskij [2]) which were obtained by the vapour pressure method. The data reported by Fedorova [1]) agree well for the solidus curve but show remarkable deviations for the liquidus curve. The departure with respect to our points is appreciable for a concentration of about 70% CH_4 where the corresponding temperature

TABLE I

Freezing and melting temperatures for the N_2–CH_4 system

mole % CH_4	T^f °K	T^m °K	mole % CH_4	T^f °K	T^m °K
0.0	63.1	63.1	40.0	69.4	—
5.0	62.9	62.6	45.0	71.2	62.8
10.0	62.8	62.5	49.0	72.5	—
13.4	62.9	62.5	50.0	72.8	62.6
15.7	62.9	62.6	50.0	72.6	—
18.2	62.6	62.5	51.0	73.2	—
20.7	62.8	62.4	54.8	74.5	62.8
21.3	62.8	62.4	58.0	75.3	—
22.5	63.2	62.6	64.5	77.3	—
25.0	63.4	62.6	69.6	79.4	—
25.0	63.4	62.4	70.4	79.3	—
28.2	64.6	62.8	73.8	80.6	73.8
28.5	64.3	62.7	80.3	82.9	77.8
31.0	66.0	62.7	84.6	84.5	—
34.5	66.8	62.8	85.3	84.8	80.7
38.8	68.7	62.8	87.2	85.5	—
39.5	69.1	—	96.3	89.0	87.9
			100.0	90.6	90.6

difference is about 7°K; obviously, there was some difficulty with localization of the freezing points in regions II and III because the tail of the heat capacity curves does not indicate with sufficient accuracy the end of the fusion process (see figs. 9 and 10).

The vapour pressure method provides of course, information on the vapour pressure of the liquid mixture of constant concentration; these corresponding data are given only graphically in fig. 14. The vapour pressure of the mixtures saturated with solid can be read from the three-phase curve in the same figure; the smoothed values are given in table II.

TABLE II

Three-phase line data

T °K	p_{sat} cm Hg	T °K	p_{sat} cm Hg	T °K	p_{sat} cm Hg
60	5.2	70	20.5	80	44.8
62.5	8.1	72.5	26.6	82.5	51.1
65	11.5	75.	34.0	85	47.4
67.5	15.8	77.5	39.8	87.5	36.2

It was interesting to get some idea about the solid-solid phase equilibrium part below the eutectic temperature down to the nitrogen transition point at 35.5°K. Solid methane exhibits a face centered cubic structure down to the hydrogen temperature[16][17], while β-nitrogen has a hexagonal structure below its triple point[18] which changes into α-nitrogen with a cubic lattice at the transition temperature[17][18][19]. Therefore, if the solidus line would extend to the nitrogen transition point, the $S_\alpha - S_\beta$ equilibrium lens would converge at 35.5°K. In order to obtain this additional information we performed some heat capacity measurements using the apparatus *b* cooled with cold hydrogen gas to obtain the few points on the $T - x$ diagram given in fig. 15. Figs. 7 and 9 give examples of each transition. As the diffusion in the solid phase is rather slow, the accuracy of these points depends considerably upon the time allowed during the measurements for the system to attain an actual thermodynamic equilibrium.

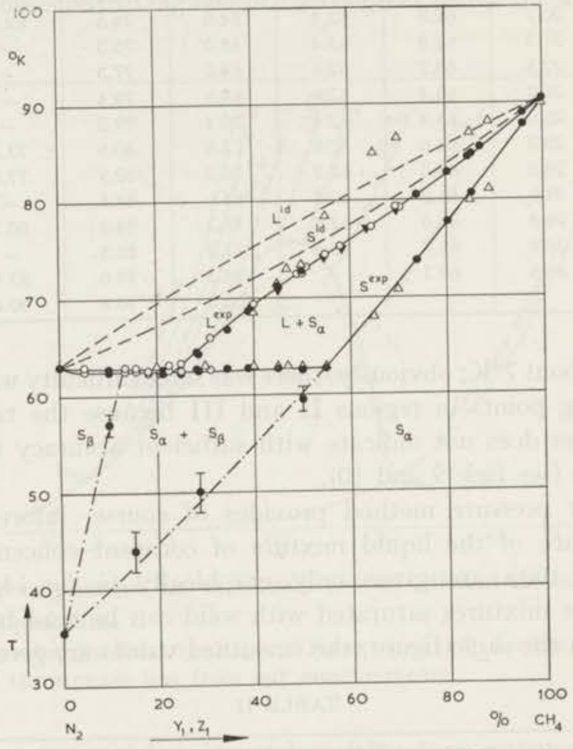

Fig. 15. The melting diagram for the N_2–CH_4 system.

- - - - - - ideal curves for solid-liquid equilibrium
○ measurements with apparatus (*a*)
● measurements with apparatus (*b*)
△ measurements of Fedorova[1])
▼ measurements of Fastovskij and Krestinskij [2])
—·—·— solid-solid phase equilibrium.

6. *Discussion*. In order to analyse the experimental results we shall discuss successively the usual thermodynamic approaches concerning the solid-liquid phase equilibrium. First we shall consider the equilibrium between the liquid solution and the pure solid.

The second part of this section will deal with equilibrium between the liquid solution in equilibrium with mixed crystals.

For the condition of equilibrium between a liquid mixture and the pure solid phase one obtains from the Gibbs equality of partial chemical potentials of the solute in both phases the well known equation found in textbooks on thermodynamics[21][22][23]:

$$-\ln y_1\gamma_1 = \frac{\Delta h_1^{0f}}{R}\left(\frac{1}{T}-\frac{1}{T_1^{0f}}\right) + \frac{c_{p1}^{0L}-c_{p1}^{0S}}{R}\left(\ln\frac{T_1^{0f}}{T}+1-\frac{T_1^{0f}}{T}\right) \quad (1)$$

wherein the conventional notation is used: y_1 mole fraction of the solute in the liquid; γ_1 activity coefficient of the solute in the liquid; Δh_1^{0f} molar heat of fusion of the pure solute at its triple point T_1^{0f}; R the universal gas constant; c_{p1}^{0L} and c_{p1}^{0S} are the heat capacities at constant pressure of the pure substance 1 in the liquid and solid states at the triple point T_1^{0f}; the subscript 1 refers to methane and the subscript 2 refers to nitrogen. The right hand side terms of eq. (1) are obviously the result of the integration of the molar heat of fusion of the species 1 divided by RT^2. The difference of the heat capacities is treated as constant.

The formula (1) is simplified if we neglect the second term of the right hand side and assume the validity of Raoult's law. The activity coefficient, γ_1, thus equals 1 and we obtain the equation of Schröder[24] for the ideal solubility of a solid, y_1^{id}, in an ideal liquid mixture:

$$\ln\frac{1}{y_1^{id}} = \frac{\Delta h_1^{0f}}{R}\left(\frac{1}{T}-\frac{1}{T_1^{0f}}\right). \quad (2)$$

In the case of a non ideal liquid mixture we need to calculate the activity coefficient which is usually described analytically by means of a series expansion of $RT \ln \gamma_1$ in powers of y_2[23][25]. The first term of such an expansion is always quadratic, wy_2^2, where w is independent of temperature and concentration. With the restriction to this quadratic term only, the formula (1) can be rewritten as follows:

$$\ln(y_1^{id}/y_1) = (w/RT)\, y_2^2. \quad (3)$$

The constant w is the same as the constant b in the article of Hildebrand[26] introducing his concept of regular solution. The use of the same constant w has later been justified in the statistical theories of molecular physics[27]. The same constant w, frequently written as $Q_{M\infty}$, was termed as a differential molar heat of mixing of a rare gas in an infinitely diluted solvent[5].

Another more general formula introduced by Hildebrand[22] uses the volume concentration φ_2 in place of the molar concentration y_2:

$$\ln\frac{y_1^{id}}{y_1} = \frac{v_1^0(\delta_1-\delta_2)^2}{RT}\,\varphi_2^2 \quad (4)$$

where v_1^0 is the molar volume of the solute 1 and δ_1 and δ_2 are the solubility parameters calculated from the energy of vaporization. Fastovskij and

Krestinskij[2]) compared the above mentioned theory with their measurements of the liquidus curve in the concentration range (45–70)% CH_4. They probably assumed that the solid phase would be formed by pure solid methane which crystallizes in the cubic face centered system with $a = 5.89$ Å[16]) [17]) [19]), while β-nitrogen crystallizes in a hexagonal system with $a = 4.034$ Å and $c = 6.59$ Å[18]). Below 35.5°K, α-nitrogen has a cubic lattice with $a = 5.65$ Å[19]) [20]). Their conclusion was that their experimental data significantly differ from the ideal solubility (eq. (2)). Their data could not be correlated with the regular solution theory according to eq. (3). On the other hand they believed that the more accurate relation, eq. (4), for the solution with unlike molar volumes could satisfactorily represent their data in their limited range of concentration.

As our measurements provided the liquidus curve in the whole concentration ranges we performed the above mentioned calculations again which proved once more the non applicability of the eqs. (1), (2) and (3) for the investigated $N_2 - CH_4$ system. By means of eq. (4) we calculated the difference of the solubility parameters; $(\delta_1 - \delta_2)$ proved to be strongly temperature dependent and the relatively large value of $(\delta_1 - \delta_2)$ did not agree with the predictions derived from the latent heats of evaporation for both components. The conclusion is, therefore, that none of the above formulae can give a right order of magnitude for the solubility under the assumption that pure solid methane is in equilibrium with the liquid solution. The occurrence of mixed crystals of N_2 in the CH_4-lattice along the solidus curve makes it necessary for the calculation to take into account also the change of the Gibbs function during the mixing process in the solid phase. We shall write the change of the Gibbs functions $G^L{}_m$ for mixing in the liquid phase, and $G^S{}_m$ for the change on mixing in the solid phase, with respect to the same reference state which will be here the system of n_1 moles of pure liquid CH_4 and n_2 moles of pure liquid N_2 at the temperature T:

$$G^L{}_m = \sum_{i=1}^{2} n_i{}^L \, RT \ln y_i \gamma_i{}^L \tag{5}$$

$$G^S{}_m = \sum_{i=1}^{2} n_i{}^S \, RT \ln z_i \gamma_i{}^S + \sum_{i=1}^{2} n_i \Delta h_i{}^{0f} (T/T_i{}^{0f} - 1) \tag{6}$$

wherein y_i and z_i are the liquid and solid molar concentration of the component i; $\gamma_i{}^L$ and $\gamma_i{}^S$ are the activity coefficients and $\Delta h_i{}^{0f}$ is the molar heat of fusion of the pure component i at its triple point $T_i{}^{0f}$. Following the method of Gibbs[28]) we plot $G^L{}_m$ and $G^S{}_m$ against the concentration for each temperature and the common tangent provides the equilibrium compositions for the respective phases. Such a graphical method gives conveniently rapid approximate results in the case of the equilibrium between an ideal liquid and an ideal solid solution (i.e. when $\gamma_i{}^L = \gamma_i{}^S = 1$ for $i = 1, 2$). In the case of the equilibrium between a regular liquid and regular solid solution, (i.e.

$RT \ln \gamma_1^{\mathrm{L}} = w^{\mathrm{L}} y_2^2$ and $RT \ln \gamma_1^{\mathrm{S}} = w^{\mathrm{S}} z_2^2$) it is necessary to determine the two parameters w^{L} and w^{S} respectively by trial and error from the known experimental data at a single temperature. The subsequent comparison of the determined compositions at all other temperatures reveals whether the concept of regular solution adequately represents the behaviour of the system under consideration.

For exact work we must differentiate eqs. (5) and (6) in order to obtain the equality of the partial chemical potentials in both phases for both components:

$$RT \ln y_1 \gamma_1^{\mathrm{L}} = RT \ln z_1 \gamma_1^{\mathrm{S}} + \Delta h_1^{0\mathrm{f}} (T/T_1^{0\mathrm{f}} - 1) \qquad (7)$$

$$RT \ln y_2 \gamma_2^{\mathrm{L}} = RT \ln z_2 \gamma_2^{\mathrm{S}} + \Delta h_2^{0\mathrm{f}} (T/T_2^{0\mathrm{f}} - 1). \qquad (8)$$

Using the abbreviations

$$\lambda_1 = (\Delta h_1^{0\mathrm{f}}/R)(1/T - 1/T_1^{0\mathrm{f}}) \qquad (9)$$

$$\lambda_2 = (\Delta h_2^{0\mathrm{f}}/R)(1/T - 1/T_2^{0\mathrm{f}}) \qquad (10)$$

we can solve the equations (7) and (8) for $y_2 = 1 - y_1$ and $z_2 = 1 - z_1$ in terms of γ_i's:

$$y_2 = \frac{\mathrm{e}^{\lambda_1} \gamma_1^{\mathrm{L}} \gamma_2^{\mathrm{S}} - \gamma_1^{\mathrm{S}} \gamma_2^{\mathrm{S}}}{\mathrm{e}^{\lambda_1} \gamma_2^{\mathrm{S}} \gamma_1^{\mathrm{L}} - \mathrm{e}^{\lambda_2} \gamma_1^{\mathrm{S}} \gamma_2^{\mathrm{L}}} \qquad (11)$$

$$z_2 = \frac{\mathrm{e}^{\lambda_1} \gamma_1^{\mathrm{L}} \gamma_2^{\mathrm{L}} - \gamma_1^{\mathrm{S}} \gamma_2^{\mathrm{L}}}{\mathrm{e}^{\lambda_1 - \lambda_2} \gamma_2^{\mathrm{S}} \gamma_1^{\mathrm{L}} - \gamma_1^{\mathrm{S}} \gamma_2^{\mathrm{L}}}. \qquad (12)$$

In the case of an ideal system these equations go over into the equations of van Laar[29]). The semigraphical method of Seltz[30]) using fugacities following the Lewis-Randall rule, leads also to the formula of van Laar. If the activity values are known another generalized graphical treatment on the basis of activities was proposed and discussed by Seltz[31]) and Scatchard[32]).

If values of $\Delta h_1^{0\mathrm{f}} = 224$ cal/mole and $\Delta h_2^{0\mathrm{f}} = 172$ cal/mole are used the ideal solution theory gives by means of the above mentioned method the broken curves shown in fig. 15. The same set of curves L^{id} and S^{id} was used for the calculations of the ideal three-phase line in fig. 14. The disagreement, however, suggests a large deviation from Raoult's law.

The adjustment of the two parameters w^{L} and w^{S} at about 75°K gave the values 120 ± 20 cal/mole and 200 ± 30 cal/mole respectively. For other temperatures of the melting region the concentrations y_1^{calc} and z_1^{calc} calculated by means of eqs. (11) and (12) can be compared with the experimental smoothed values y_1^{exp} and z_1^{exp}.

From an inspection of table III we see that the agreement is satisfactory in view of the accuracy of the measurements (2%). The calculated compositions are reproduced within the uncertainty in the parameters w^{L} and w^{S}.

TABLE III

Comparison between calculated and experimental results				
T °K	$100y_1^{\text{exp}}$	$100y_1^{\text{calc}}$	$100z_1^{\text{exp}}$	$100z_1^{\text{calc}}$
90.6	100.0	100.0	100.0	100.0
85	86.0	86	91.8	94
80	72.0	72	84.1	87
75	56.8	57	76.0	79
70	41.9	42.5	67.6	69
65	29.1	29	58.8	57.5
63.1	24.4	22	55.6	53

The value of the quantity $w^{\text{S}} = 200$ cal/mole indicates a critical temperature of demixing $T_c = w^{\text{S}}/2R = 50$°K. From the above considerations one concludes that the solid-liquid equilibrium of the N_2–CH_4 system can be described on the basis of the regular theory assumptions.

REFERENCES

1) Fedorova, M. F., J. expt. theoret. Phys. U.S.S.R. **8** (1938) 425; Acta Physicochimica U.R.S.S. **10** (1939) 539.
2) Fastovskij, V. G. and Krestinskij, Y. A., J. phys. Chem. U.S.S.R. **15** (1941) 525.
3) Roozeboom, H. W., Die heterogenen Gleichgewichte, 2.Heft (Friedrich Vieweg und Sohn, Braunschweig 1904).
4) Bloomer, O. T. and Parent, J. D., Inst. of Gas Technology, Res. Bull **17** (1952).
5) Stackelberg, M. V., Heinrichs, M. and Schulte, W., Z. physik. Chem. **170** (1934) 262.
6) Verschoyle, T. T. H., Trans. roy. Soc. (London) **230** (1931) 189.
7) Heastie, R., Proc. phys. Soc. **73** (1959) 490.
8) Din, F., Goldman, K. and Monroe, A. G., 9th Internat. Conf. on Refrigeration, Paris (1955).
9) Ruhemann, M. and Lichter, A., Phys. Z. Sowjetunion **6** (1935) 139.
10) Ruhemann, M. Lichter, A. and Komarov, P., Phys. Z. Sowjetunion **8** (1935) 326.
11) Tamman, G., Z. anorg. Chem. **37** (1903) 303.
12) Stackelberg, M. V. and Quatram. F., Z. Elektrochem. **42** (1936) 552.
13) Veith, H. and Schröder, E., Z. phys. Chem **179** (1937) 16.
14) Long, H. M. and Di Paolo, F. S., Proc. of the Meeting of Commission I of the Internat. Institute of Refrigeration, Delft, The Netherlands (1958).
15) Heastie, R. and Lefèbvre, C., Proc. phys. Soc. **76** (1960) 180.
16) Mooy, H. H., Commun Kamerlingh Onnes Lab., Leiden No. 216*a* (1931).
17) Mooy, H. H., Commun. Leiden No. 213*d*. (1931) 35.
18) Taconis, K. W., Thesis, Leiden (1938).
19) Mooy, H. H., Thesis, Leiden (1931).
20) Vegard, L., Z. phys. **58** (1929) 497.
21) Guggenheim, E. A., Thermodynamics (North-Holland Publishing Company, Amsterdam 1957) 3rd. ed.
22) Hildebrand, J. H. and Scott, R. L. The solubility of non electrolytes (Reinhold Publ. Corp., New York 1950).
23) Prigogine, I. and Defey, R., Thermodynamique chimique (Editions Desoer, Paris, 1950).
24) Schröder, J., Z. physik. Chem. **11** (1893) 449.
25) Hála, E., Pick, J., Fried, V. and Vilím, O., Vapour-liquid equilibrium (Pergamon Press, London 1958).
26) Hildebrand, J. H., J. amer. chem. Soc. **51** (1929) 66.

27) **Prigogine, I.**, Molecular theory of solutions (Noth Holland Publ. Comp., Amsterdam 1957).
28) **Gibbs, J. W.**, Collected Works (Longmans, Green and Co., New York 1906 p. 118).
29) **Van Laar, J. J.**, Chemische Thermodynamik (Dresden und Leipzig, Steinkopff 1938).
30) **Seltz, H.**, J. amer. chem. Soc. **56** (1934) 307.
31) **Seltz, H.**, J. amer. chem. Soc. **57** (1935) 391.
32) **Scatchard, G.**, J. amer. chem. Soc. **62** (1940) 2426.

CHAPTER III

SOLID-GAS EQUILIBRIUM OF THE BINARY OXYGEN-HYDROGEN SYSTEM

Synopsis

The equilibrium between the solid and gas phases of mixtures of oxygen and hydrogen has been studied using a modified flow method. The measurements have been performed at pressures of 5,10, and 15 atm and at temperatures from the triple point temperature of oxygen (54.4°K) down to 40°K. The agreement between theory and experiment proved to be satisfactory. The concentration of oxygen in the vapour phase down to 1 p.p.m. could be determined by means of freezing out the oxygen at 20°K.

1. *Introduction*. Soon after the accomplishment of experiments on the solid-gas equilibrium of the N_2–H_2 and CO–H_2 systems¹), the need for an analogous set of data for the O_2–H_2 system became urgent. The same experimental apparatus could, in principle, be used as in the previous case, and the same basic theory developed for the solid-gas equilibrium, was available.

The excellent agreement at that time between the measured concentrations of the system N_2–H_2 and the calculated data suggested that an analogous calculation of the solubility of the solid oxygen in the gaseous hydrogen would suffice. Another reason for dropping the experimental determinations was the possible danger when working with relatively large quantities of a mixture of oxygen and hydrogen needed for the flow method with our standard large equilibrium vessel. The theoretical curves were calculated for the pressures 5, 10, 15, 25 and 50 atm in the temperature range below the triple point of oxygen down to about 35°K.

More recently, a series of experiments concerning the solid-liquid equilibrium of the binary systems N_2–H_2 and O_2–H_2 has been started. For a better understanding of these results, the directly measured data on the solid-gas equilibrium of the O_2–H_2 system were needed in the neighbourhood of the critical temperature of hydrogen. The theory in this region is not sufficiently exact. Moreover, the solubilities of O_2 and N_2 were of different orders of magnitude near the liquid region.

We decided, therefore, to perform the direct measurements on the solid-gas system of O_2–H_2 with another apparatus. A description of the experimental method will be given in the next section. The third section contains the experimental results, which are subsequently discussed in the last section. A brief account on this work has already been given in a review article in Progress in low temperature physics III [2]).

2. *Experimental method.* When using our standard equilibrium vessel designed for the application of the flow method we would have needed large quantities of mixtures of oxygen and hydrogen prepared and stored in high pressure cylinders before every run. In order to avoid any possible occurrence of explosion we decided, therefore, to use another small equilibrium vessel which was primarily designed for the investigation of the solubility of solids in liquids, with some modification of the manipulation procedure.

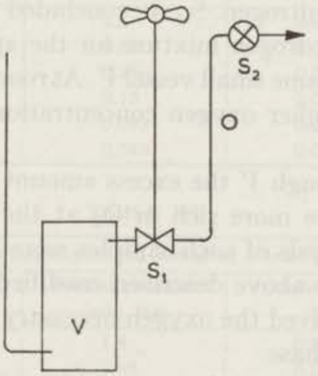

Fig. 1. The apparatus.

The equilibrium vessel V (see fig. 1) was provided with the inlet capillary I and the outlet capillary O. The bellows type valve S_1 was operated at low temperature and could withstand pressures up to 20 atm. No mixture of oxygen and hydrogen was prepared before the run: we condensed first a very small known amount of pure oxygen in the vessel V and then added subsequently pure gaseous hydrogen. As soon as the equilibrium conditions under the required pressure and temperature had been attained, the sampling through the valve took place, and the sample was subsequently analyzed. Such a modified static method gave values of the oxygen content in the vapour, which were of an order of magnitude less than the expected calculated solubilities. The explanation of this effect was indeed as suspected: due to the small volume of the equilibrium vessel, the expansion of the gas under pressure, when sampling, caused an observable decrease of temperature resulting in an additional precipitation of the already dissolved solid in the vapour; the low equilibrium pressure used ($<$ 20 atm.) dropped far below the stationary pressure during the sampling manipulation.

In order to avoid the difficulties of sampling, the above described procedure was modified in a kind of flow method wherein the pure hydrogen gas flows stationary through the inlet capillary I and passes the equilibrium vessel at the required temperature and at the constant pressure through the valve S_1 to the valve S_2 where the pressure is reduced. The oxygen was again solidified in V with closed valve S_1 before starting the run, and the properly adjusted flow allows afterwards the saturation of the pressurised gas. The sampling line is connected to the outlet capillary O behind the valve S_2. The sampling takes place through the outlet capillary at room temperature when a stationary flow at equilibrium is attained without any change of the equilibrium concentration.

From the results obtained by the above explained method we learned that the solubility of oxygen in gaseous hydrogen is nearly 10 times less than the solubility of nitrogen. So we concluded that we could use even a very diluted oxygen-hydrogen mixture for the application of the standard flow method using the same small vessel V. At room temperature we prepared mixtures of slightly higher oxygen concentration than the expected equilibrium concentration.

During the flow through V the excess amount of oxygen is then precipitated from the mixture more rich in O_2 at the equilibrium pressure and temperature. The analysis of such samples were in full agreement with the results obtained by the above described modified flow method wherein the pure hydrogen gas received the oxygen necessary for equilibrium conditions from the excess solid phase.

For the analysis of the samples, we again applied the method of freezing out the condensable component at 20°K. This method[1][2]) uses a single freezing trap and requires about one half litre of gas at S.T.P. conditions. As the presence of parasitic nitrogen in hydrogen or in oxygen gas used in our experiments could effect the results, much care has been given to the purification of the gases. The hydrogen gas was purified by means of a charcoal trap at liquid nitrogen temperature so that the condensable impurities were less than 10^{-2} p.p.m. A check was frequently made that the condensable component in the gaseous sample consisted only of oxygen. This was achieved by means of the explosion method in a McLeod gauge where added hydrogen has been burned with the collected oxygen from the sample.

3. *Results.* Tables I, II and III contain the partial pressures of oxygen in hydrogen and the composition of the vapour phase in equilibrium with the solid phase at 15, 10 and 5 atm respectively, at the temperatures varying from the triple point of oxygen down to about 40°K.

TABLE I

Oxygen-hydrogen isobar at 15 atm.		
Temperature (°K)	Partial pressure (mm Hg)	Concentration (%)
53.0	1.4	0.013
52.0	0.91	0.0080
50.9	0.75	0.0065
49.7	0.83	0.0073
48.9	0.47	0.0047
48.0	0.31	0.0028
46.0	0.16	0.0014
44.0	0.090	0.00079
40.0	0.013	0.00011

TABLE II

Oxygen-hydrogen isobar at 10 atm.		
Temperature (°K)	Partial pressure (mm Hg)	Concentration (%)
54.7	2.6	0.035
52.0	0.85	0.011
49.1	0.29	0.0038
47.1	0.15	0.0020
45.8	0.093	0.0012
44.0	0.049	0.00063

TABLE III

Oxygen-hydrogen isobar at 5 atm.		
Temperature (°K)	Partial pressure (mm Hg)	Concentration (%)
54.7	1.8	0.048
52.2	0.65	0.016
49.1	0.021	0.0056
47.1	0.083	0.0022
45.8	0.066	0.0017
44.0	0.036	0.00097
42.0	0.0086	0.00022
41.4	0.0076	0.00020
40.0	0.0036	0.00012

The data are graphically presented in the usual graphs. Fig. 2 shows the increase of the partial pressure as a function of the temperature.

The ratio of the partial pressure to the vapour pressure of the pure solid oxygen at different temperatures (i.e. the so-called enhancement factor *f*) is given as a function of pressure in fig. 3.

Fig. 4 gives the concentration as a function of temperature at constant pressure. By means of cross-plotting one can obtain fig. 5 showing the concentration as a function of the pressure at constant temperature.

Finally fig. 6 gives the optimum pressure corresponding to the minimum concentration as a function of temperature.

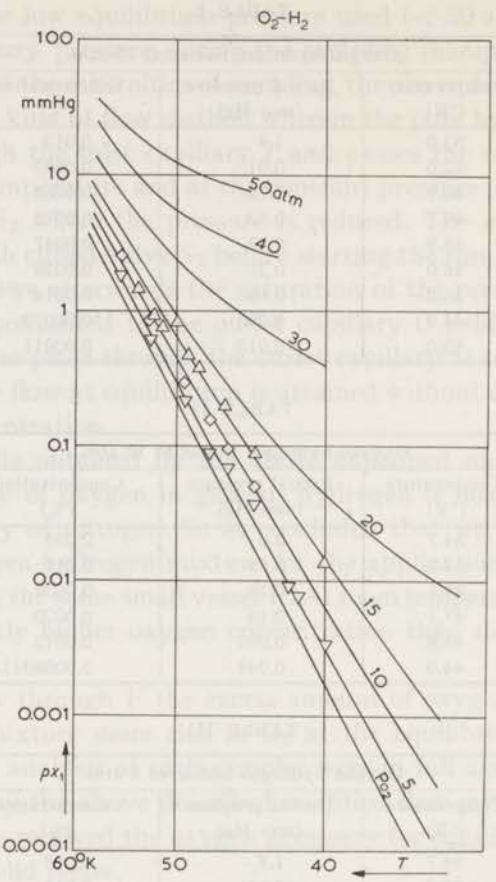

Fig. 2. The partial pressures of oxygen in hydrogen as a function of temperature at constant pressures:
▽ 5 atm, ◇ 10 atm, and △ 15 atm,
—— theoretical curves.

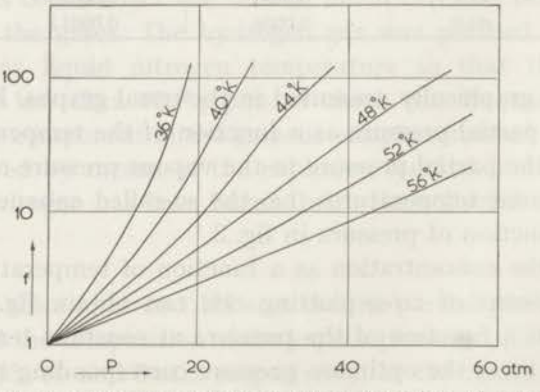

Fig. 3. The calculated enhancement factor *f* as a function of pressure for different temperatures.

4. *Discussion.* Both above mentioned experimental methods gave consistent results and therefore we did not discriminate between the

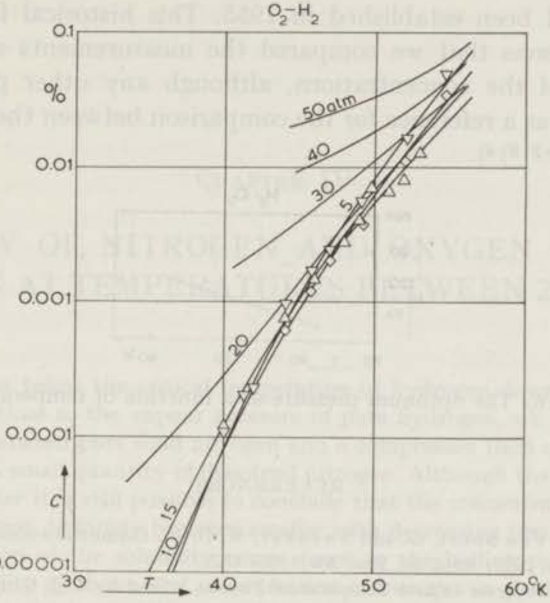

Fig. 4. The $T - x$ isobars of O_2–H_2 mixtures:
▽ 5 atm, ◇ 10 atm, and △ 15 atm,
—— theoretical curves.

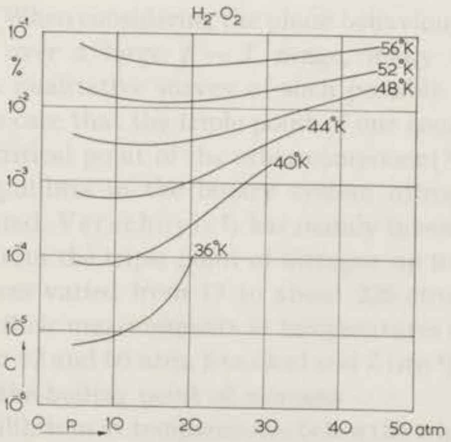

Fig. 5. The $p - x$ isotherms of H_2–O_2 mixtures.

obtained measured points when plotting them in the figs. 2 and 4. The accuracy is estimated to be 2–4% and decreases with decreasing temperature.

The full curves in figs. 2 and 4 were calculated following the formalism derived previously¹). The agreement between the measurements and the theory proves to be quite satisfactory and so the calculated predictions were fully confirmed. These calculations were already performed shortly after the theory had been established in 1955. This historical fact constitutes one of the reasons that we compared the measurements and the theory on the basis of the concentrations, although any other parameter used could be taken as a reference for the comparison between the measurements and the theory²)³)⁴).

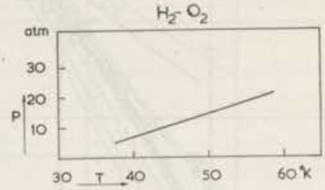

Fig. 6. The optimum pressure as a function of temperature.

REFERENCES

1) Dokoupil, Z., Van Soest, G. and Swenker, M. D. P., Communications Kamerlingh Onnes Lab., Leiden No. 297*c*; Appl. sci. Res. **A5** (1955) 182.

2) Dokoupil, Z., Progress in Low Temperature Physics, edited by C. J. Gorter (North-Holland Publishing Company, Amsterdam 1961). Vol. III, chapt. XI.

3) Reuss, J. and Beenakker, J. J. M., Commun. Leiden Suppl. No. 110*e*; Physica **22** (1956) 869.

4) Rowlinson, J. S. and Richardson, M. J., Advances in chemical Physics, edited by I. Prigogine (Inter-Science Publishers Ltd., New York, London 1959) Vol. II.

CHAPTER IV

SOLUBILITY OF NITROGEN AND OXYGEN IN LIQUID HYDROGEN AT TEMPERATURES BETWEEN 27 AND 33°K

Synopsis

At temperatures below the critical temperature of hydrogen down to about 27°K, and at pressures close to the vapour pressure of pure hydrogen, we have determined the equilibrium between pure solid nitrogen and a compressed fluid consisting mainly of hydrogen and a small quantity of dissolved nitrogen. Although the measured points show a large scatter it is still possible to conclude that the concentration of dissolved nitrogen in hydrogen definitely becomes smaller with decreasing temperature. A very rough extrapolation of the solubility curve down to the boiling point of hydrogen results in a solubility of about 10^{-8} mole fraction of nitrogen in the liquid. Using our analysis apparatus which allowed us to detect a condensable component only down to 0.2 p.p.m., we could not find any measurable solubility of oxygen in liquid hydrogen in the same $p - T$ region. The measurements have been analyzed by means of the theory of Hildebrand.

1. *Introduction.* When considering the phase behaviour of a binary system hydrogen-nitrogen over a large $p - T$ range, many different equilibria can be expected. A qualitative survey of such possible equilibria has been given earlier for the case that the triple point of one constituent component is higher than the critical point of the other component[1]).

Several phase equilibria in the binary system nitrogen-hydrogen have already been measured. Verschoyle[2]) has mainly investigated the vapour-liquid equilibrium from the triple point of nitrogen up to about 88°K, while the working pressures varied from 17 to about 225 atm. Ruhemann and Zinn[3]) carried out their measurements at temperatures of 78, 83 and 90°K, at pressures between 12 and 50 atm. Steckel and Zinn[4]) worked at temperatures higher than the boiling point of nitrogen.

The solid-gas equilibrium at temperatures below the triple point of nitrogen down to the critical region of hydrogen was investigated by a Leiden group[1]). The measurements on the same solid compressed-fluid equilibrium at pressures higher than the critical pressure of hydrogen were extended to temperatures below the critical temperature of hydrogen by Petit[5]). Additional measurements on the liquid-gas equilibrium at low pressures and at temperatures near the triple point of nitrogen were recently performed by Omar and Dokoupil[6]).

The question of the solubility of nitrogen in liquid hydrogen has frequent been asked by the cryogenic workers. In the last few years it became urgent to collect additional information about the behaviour of the important technical gases and the properties of their mixtures. In the following sections we shall describe our measurements on the solubility of nitrogen in liquid hydrogen. The experiments cover the region of temperature below the critical temperature of hydrogen down to about 27°K, as the concentrations below this temperature proved to be too small for our means of detection. In the second section we shall discuss some general properties of the solubility of a solid in a liquid, which result from the qualitative shape of the phase diagrams. The third section contains a description of the apparatus and the experimental procedure. Section four contains the experimental results from which the difference of the solubility parameters is derived. The fifth and last section includes a discussion of the results.

2. *Phase equilibrium behaviour.* In order to introduce the definition of the solubility of nitrogen in liquid hydrogen we shall very briefly discuss the corresponding phase diagrams in the temperature range below the critical point of hydrogen.

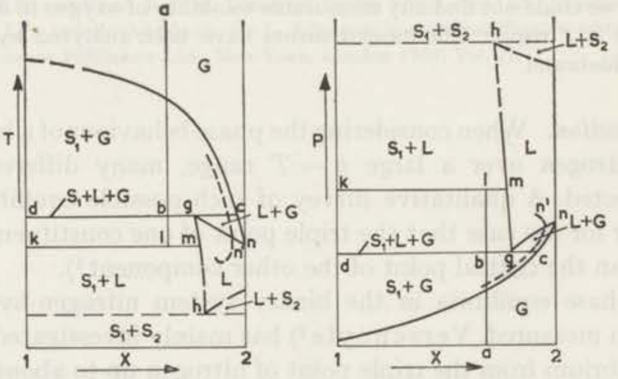

Fig. 1*a*, 1*b*. T — *x* diagram and *p* — *x* diagram of a binary mixture below the supercritical region.

The $T - x$ diagram is shown qualitatively in fig. 1*a* for the case that the pressure is kept constant at some value below the critical pressure of hydrogen. In fig. 1*b* the $p - x$ diagram is drawn for some fixed value of the temperature below the critical temperature of hydrogen. The symbol G is used to indicate the gaseous phase, L for the liquid phase and S for the solid phase. The subscript 1 refers to the solute and the subscript 2 to the solvent. When constructing the two diagrams the concentration scale in the neighbourhood of the hydrogen axis has been enlarged in order to show easily the interpenetration of the equilibrium loops $S_1 + G$ and $S_1 + L$. It has been assumed that the solid phase S_1, which is in equilibrium with the liquid mixture L, consists only of pure nitrogen: this assumption was similarly introduced in the case of equilibrium between solid nitrogen and the gaseous mixture at temperatures higher than the critical point of hydrogen[1]). The region comprising the assumed eutectic part of the melting diagram in the neighbourhood of the triple point of hydrogen, which lies far below our range of temperatures, is indicated by dashed lines in both qualitative diagrams 1*a* and 1*b*.

As we are below the critical point of hydrogen both homogeneous regions G and L are separated from each other by the liquid-gas equilibrium loop which is extended to the hydrogen axis. Above the critical point of hydrogen both regions would be connected because the $L + G$ loop does not touch the hydrogen axis at the point n (see the broken line). In both figs. 1*a* and 1*b* we indicated the strictly isobaric and isothermal melting curves $h - m - g$ which form a boundary of the two phase equilibrium region $S_1 + L$; for such a corresponding equilibrium condition the coexistence of both phases is characterized by the connodal $k - m$. There is no gaseous phase at all above the compressed fluid under such conditions of two degrees of freedom.

In contrast to the above mentioned definition of an isothermal or isobaric solubility along the boundary curves $h - m - g$, one frequently considers the univariant equilibrium $S_1 + L + G$ along the three phase connodals $d - g - c$. In this case the gaseous mixture given by point c is in equilibrium with the saturated liquid, g, under its own saturation pressure; point d refers to the excess pure solid nitrogen coexisting in equilibrium with the liquid and gas phases.

From the diagrams in figs. 1*a* and 1*b* it follows immediately that the solubility of nitrogen in liquid hydrogen is larger than its solubility in the gaseous phase. Further, we can expect that the pressure dependence of the solubility in the liquid phase should be small as compared with the pressure dependence in the gaseous phase. In other words the distance of the melting line ($g - m - h$ in fig. 1*a*) from the hydrogen axis would not be very sensitive to different pressures.

In our measurements we have made an attempt to determine the melting line from 32°K down to about 27°K at pressures near the saturated pressure of the liquid hydrogen.

3. *Experimental method.* From the discussion in the previous section concerning the solubility diagrams, it becomes directly evident that we cannot apply a dynamic flow method or a circulation method to perform our measurements; the gaseous sample leaving the apparatus would contain less dissolved nitrogen than the saturated liquid under the equilibrium

conditions. Therefore, we designed an apparatus adopted for the application of the static method. Fig. 2*a* represents a schematic diagram of the apparatus while fig. 2*b* shows the detailed construction.

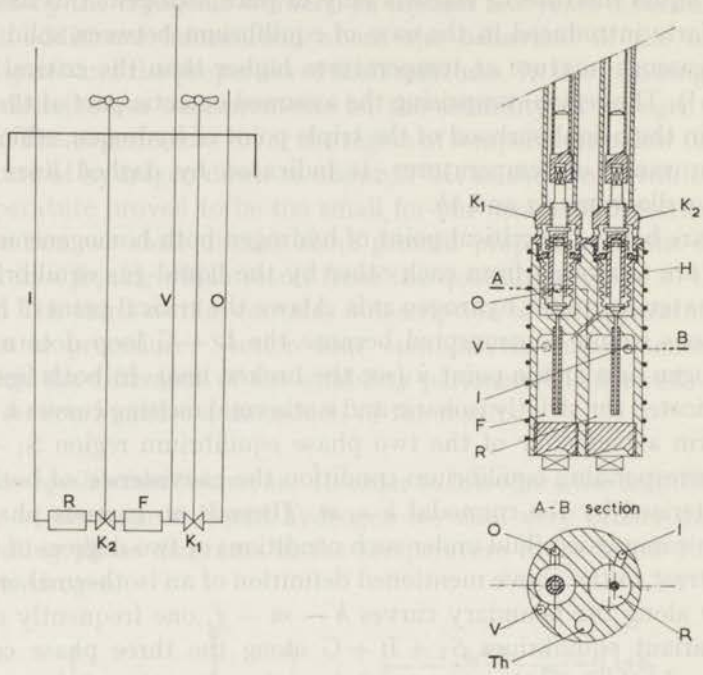

Fig. 2*a*, 2*b*. Schematic and detailed diagrams of the apparatus.

When using the static method we withdraw discontinuously and rapidly a sample of liquid out of the equilibrium vessel by opening the valve K_2 which is placed necessarily at the same low temperature as the main equilibrium vessel R; otherwise if K_2 would be at room temperature, we would not get an actual representative sample due to the higher temperature of the outlet capillary. In order to investigate the influence of the rapid decrease of pressure when sampling, we put an additional equilibrium cell F behind K_2, which can be evacuated through the capillary V. Another low temperature valve K_1 separates the high pressure part of the apparatus from the sampling capillary O.

To perform the experiment, one could proceed as follows: first we prepare a gaseous mixture of hydrogen containing nitrogen (or oxygen) in excess of the expected equilibrium composition; further we introduce this gaseous mixture into the previously evacuated equilibrium vessel kept at the required temperature; after the pressure is built up, we wait until equilibrium conditions are established in order to perform the subsequent sampling. Following such a filling procedure given by the path $a - b - l$ on the corresponding diagrams in fig. 1*a* and 1*b*, we can make two conclusions: for a small initial nitrogen excess in the gaseous mixture we could loose so much nitrogen in the part of the capillary close to R during the slow filling period that the liquid has not enough solute left for the saturation; for a large initial nitrogen excess in the gaseous mixture, blocking of the filling capillary would easily occur. We modified, therefore, the above described filling procedure in the following way: we first fill the apparatus with a small known amount of nitrogen and then cool down the apparatus slowly enough to condense the solid nitrogen in R; then we add hydrogen up to the required pressure so that the liquid completely fills the vessel R. The liquid (or fluid) phase gets saturated by the excess available solid nitrogen. When equilibrium is reached, the liquid is transferred through K_2 into F. After the equilibrium conditions are restored, the sample is rapidly taken off through K_1.

The volumes of R and F are about 12 cm^3. The stainless steel bellows in the valves K_2 and K_1 proved to be superior to the tombac bellows. All the different parts of the apparatus with the exception of the thermometer and the heating coils were constructed in a massive brass block.

The apparatus could withstand pressures up to 20 atm, and it was cooled by means of a stream of cold hydrogen gas evaporating from a bath of liquid hydrogen kept at some distance below the brass block. The analysis of the samples were performed by passing the mixture through a capillary surrounded by liquid hydrogen. When all the nitrogen is frozen out, the hydrogen gas left was then pumped out completely. After warming up the system, the pressure effectuated by the trapped nitrogen, was measured with McLeod gauge, and gave a measure for the nitrogen concentration. The analysis of very small concentrations was improved by collecting more solid nitrogen frozen out from two or three successive fillings with the same sample in the freezing-out capillary. After the last cycle we could determine the total amount of trapped nitrogen and consequently the corresponding concentration. Such an analysing procedure naturally becomes more complicated and less accurate. The lowest possible concentration which could be detected by this procedure was about 0.2 p.p.m.

The McLeod gauge in the analysis system was modified as described by Tompkins and Young[7]) for the analysis of a $N_2 + O_2$ mixture, using the method of combustion in presence of a previously known small quantity of hydrogen or carbon monoxide. Using this method we could determine whether the collected nitrogen after the performance of the analysis was contaminated by oxygen, or conversely if the trapped oxygen contained nitrogen. This procedure proved to be quite satisfactorily.

4. *Experimental results.* Hydrogen and nitrogen gases were supplied from the laboratory stock; the purity of the hydrogen was better than 99.9% while that of nitrogen gas was 99.8%. As the purity of hydrogen plays

TABLE I

Solubility of nitrogen in liquid hydrogen

Temperature (°K)	Mole concentration	Pressure (atm)	Temperature (°K)	Mole concentration	Pressure (atm)
32.5	7.0×10^{-6}	15.3	28.5	4.9×10^{-6}	—
32.0	2.6×10^{-5}	17.0	28.0	5.4×10^{-6}	11.0
32.0	1.6×10^{-5}	14.5	27.5	1.7×10^{-6}	13.2
32.0	6.8×10^{-6}	13.0	27.5	1.1×10^{-6}	11.0
31.5	8.0×10^{-6}	13.5	27.0	1.1×10^{-6}	8.9
30.3	9.4×10^{-6}	12.2	27.0	1.1×10^{-6}	7.5
30.3	7.4×10^{-6}	12.0	27.0	2.5×10^{-6}	7.4
30.0	5.5×10^{-6}	10.0	27.0	1.8×10^{-6}	7.0
29.5	4.0×10^{-6}	11.0	27.0	2.5×10^{-6}	6.8
29.2	4.2×10^{-6}	12.0	27.0	2.7×10^{-6}	6.0
29.5	6.6×10^{-6}	11.0	26.5	1.4×10^{-6}	13.5
29.0	7.4×10^{-6}	11.0	26.5	4.0×10^{-7}	10.0
29.0	3.8×10^{-6}	9.5	26.5	9.5×10^{-7}	8.2
28.5	3.5×10^{-6}	11.7	26.3	4.4×10^{-7}	16.5
28.5	4.0×10^{-6}	10.0	26.3	5.4×10^{-7}	6.0

an important rôle in our experiment, very pure hydrogen gas was needed. The hydrogen was purified by passing it through a charcoal trap kept at the boiling temperature of liquid nitrogen. **Brilliantov** and **Fradkov**[8]) claimed to have obtained by this method hydrogen gas with less than 2×10^{-10} mole fraction impurities. When adding some hydrogen to the nitrogen gas to be purified, we could remove any traces of oxygen by leading it over the palladium catalyst. The purity of the oxygen was checked

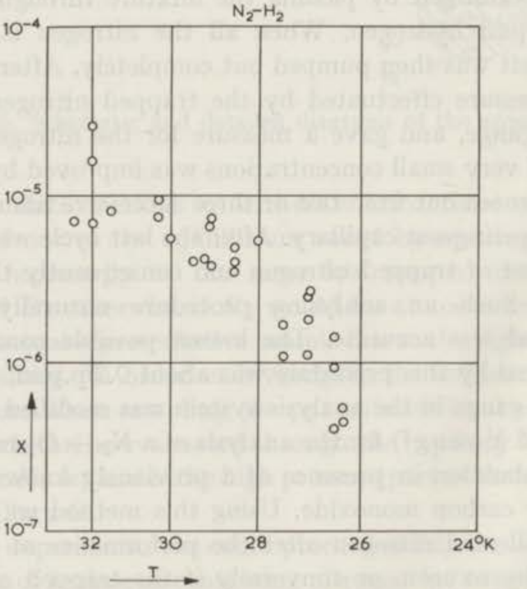

Fig. 3. Solubility of solid nitrogen in liquid hydrogen between 26 — 33°K.

afterwards by the explosion method, as explained in the preceding paragraph.

Our experimental results for the solubility of solid nitrogen in liquid hydrogen are given in table I. Fig. 3 shows the same measured points plotted on a logarithmic scale as a function of the reciprocal of the temperature. The measurements do not show any pronounced dependence of the pressure on the temperatures below 30°K. However, the solubility points show a tendency to increase with pressure as the critical temperature of hydrogen is approached. Although the points show a considerable scatter, it is possible to make a very rough extrapolation down to 20.4°K which would result in a solubility of about 10^{-8} mole fraction of nitrogen in the boiling hydrogen. The inaccuracy of the results is because of the difficulties associated with the withdrawal of the representative sample, as explained in the previous section.

In the same $p - T$ region we performed similar experiments on the oxygen-hydrogen system. Using the above-described analysis apparatus we concluded that the solubility of solid oxygen in liquid hydrogen should be less than 0.5 p.p.m.

5. *Discussion of the results.* In dealing with the solubility of pure solids in liquids, one usually encounters the following formula describing the equilibrium between the liquid mixture and a solid phase consisting only of the pure component⁹):

$$\ln y_1 \gamma_1 = \int_{T_1^{\text{of}}}^{T} \frac{h_1^{\text{L}} - h_1^{\text{S}}}{RT^2}\, \mathrm{d}T, \tag{1}$$

where y_1 is the mole fraction of component 1 in the solution, γ_1 its activity coefficient, h_1^{L} and h_1^{S} are, respectively, the enthalpy of the supercooled liquid and the enthalpy of the solid at the temperature T; T_1^{of} is the triple point of the same component 1, R is the universal gas constant. The term $h_1^{\text{L}} - h_1^{\text{S}}$ defines the molar heat of fusion which is needed to convert one mole of the solute from the solid state S into the liquid state L at the temperature T. Accurate integration of eq. (1) requires the knowledge of the variation of the heat of fusion $h_1^{\text{L}} - h_1^{\text{S}}$ with temperature.

When the heat of fusion is independent of the temperature and its value is taken equal to the molar heat of fusion Δh_1^{of} at the triple point T_1^{of}, the integration of eq. (1) gives the well-known Schröder equation¹⁰):

$$-\ln y_1\gamma_1 = \frac{\Delta h_1^{\text{of}}}{R}\left(\frac{1}{T} - \frac{1}{T_1^{\text{of}}}\right). \tag{2}$$

When applying the above-mentioned formalism to the case of our binary H_2–N_2 system we shall use the index 1 to indicate nitrogen as the solute and index 2 for liquid hydrogen as the solvent. The occurrence of the transition point for solid nitrogen at 35.5°K from the β-form to the α-form implies the necessity of splitting eq. (1) into two integrals over two temperature ranges:

$$\ln y_1\gamma_1 = \int\limits_{T_1^{\mathrm{ot}}}^{T=T_{\mathrm{trans}}} \frac{h_1^{\mathrm{L}} - h_1^{\mathrm{S}}}{RT^2}\,\mathrm{d}T + \int\limits_{T=T_{\mathrm{trans}}}^{T} \frac{h_1^{\mathrm{L}} - h_1^{\mathrm{S}}}{RT^2}\,\mathrm{d}T, \tag{3}$$

wherein T_{trans} is the transition point of solid nitrogen. Eq. (3) can be used to calculate the ideal solubility y_1^{id} of nitrogen in liquid hydrogen by putting γ_1 equal to 1. The effect of the partial molar free energy of mixing the supercooled liquid solute with the solution results in a decrease of the ideal solubility by a factor f for which Hildebrand gives[9]):

$$\ln f = \ln \frac{y_1^{\mathrm{id}}}{y_1} = \frac{v_1{}^0\varphi_2^2(\delta_1 - \delta_2)^2}{RT} \tag{4}$$

where $v_1{}^0$ is the molar volume of solid nitrogen, φ_2 is the volume fraction of liquid hydrogen in the solution: $\varphi_2 = 1$ since $y_1 \ll 1$, δ_1 is the solubility parameter of nitrogen and δ_2 is that of hydrogen.

Substituting for y_1^{id} in eq. (3) ($\gamma_1 = 1$), eq. (4) can be rewritten after rearrangement of the terms to describe the nonideal solubility of nitrogen in hydrogen:

$$\ln(1/y_1) = I_1 + I_2 + I_3 =$$

$$= -\int\limits_{T_1^{\mathrm{ot}}}^{T_{\mathrm{trans}}} \frac{h_1^{\mathrm{L}} - h_1^{\mathrm{S}}}{RT^2}\,\mathrm{d}T - \int\limits_{T_{\mathrm{trans}}}^{T} \frac{h_1^{\mathrm{L}} - h_1^{\mathrm{S}}}{RT^2}\,\mathrm{d}T + \frac{v_1{}^0(\delta_1 - \delta_2)^2}{RT}\,. \tag{5}$$

The first term I_1 in the above equation refers to β-solid N_2 and will be constant in temperature since we are interested in temperatures below the transition point. The second term I_2 refers to α-solid N_2; this term will be a function of the temperature. The last term I_3 stands for the deviation from the ideal case.

Eq. (5) enables us to calculate the solubility y_1 if all the parameters of the right-hand side of this equation are known. On the other hand, using the same equation, one can calculate the solubility parameter term $(\delta_1 - \delta_2)$ from our experimental results. As will be seen later, the major part of the solubility arises from the third term, I_3. Due to our lack of knowledge of accurate values for δ_1 and δ_2 in the temperature range of our work, it seemed justifiable to calculate the solubility parameter term $\delta_1 - \delta_2$ from our experimental results and to compare this value with the one estimated from the known values of the solubility parameters δ_1 and δ_2 at other temperatures.

From the known heat capacities of nitrogen[11]), we calculated the enthalpies of the α- and β-solid and liquid phases for the temperature region 20–80°K. The enthalpy h_1^L of a hypothetical supercooled liquid below the triple point was calculated also from the same heat capacity data. The results of these calculations are shown in fig. 4, and are in good agreement with the recently reported data of Din[12]). Now having values for h_1^L and h_1^S from fig. 4, the terms I_1 and I_2 appearing in eq. (5) can be calculated. The smoothed values for the solubility y_1 from our measurements enabled us to calculate the third term I_3. From table II it is evident that I_3, when compared with I_1 or I_2, contributes the largest part and thus accounts for the decrease of the actual solubility many thousands times less than expected for an ideal case.

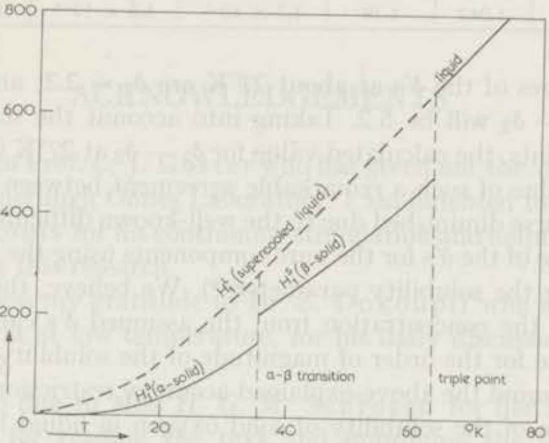

Fig. 4. Enthalpies of solid and liquid N_2.

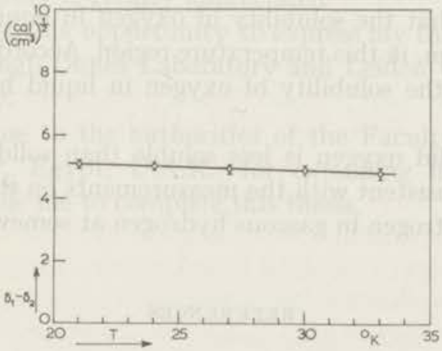

Fig. 5. Calculated $\delta_1 - \delta_2$ term.

The term $\delta_1 - \delta_2$ resulting from the above calculations is also included in table II, and is shown graphically for different temperatures in fig. 5.

The solubility parameters for pure hydrogen and nitrogen reported by Hildebrand[9]) who gave the following values: δ_2 $(H_2) = 2.5$ at 20.4°K, $\delta_1(\alpha-N_2) = 7.2$, and $\delta_1(\beta-N_2) = 6.9$. By extrapolating these data the

TABLE II

T (°K)	I_1	I_2	$I_1 + I_2$	y_1^{id}	y_1^{exp}	I_3	$\delta_1 - \delta_2$ (cal/cm^3)$^{\frac{1}{2}}$
33	0.745	0.145	0.89	4.1×10^{-1}	2.5×10^{-5}	9.71	4.80
30	0.745	0.335	1.08	3.4×10^{-1}	6.0×10^{-6}	10.6	4.85
27	0.745	0.544	1.29	2.8×10^{-1}	1.1×10^{-6}	12.4	4.95
24	0.745	0.782	1.53	2.2×10^{-1}	1.2×10^{-7}	15.9	5.04
21	0.745	1.042	1.79	1.7×10^{-1}	6.5×10^{-9}	18.9	5.15

estimated values of the δ's at about 27°K are $\delta_2 = 2.3$; and $\delta_1 = 7.5$; the difference $\delta_1 - \delta_2$ will be 5.2. Taking into account the scatter of our experimental points, the calculated value for $\delta_1 - \delta_2$ at 27°K is equal to $5.0 \pm$ $\pm$ 0.1. The value of such a remarkable agreement between experiment and theory is of course diminished due to the well-known difficulties in calculating the exact value of the δ's for the pure components using the various methods for calculating the solubility parameters[9]). We believe, therefore, that the calculation of the concentration from the assumed δ's can only provide a rough estimate for the order of magnitude of the solubility.

Keeping in mind the above-explained accuracy restrictions, we performed the calculation of the solubility of solid oxygen in liquid hydrogen for the temperature 30°K. The obtained result indicated a solubility of less than 10^{-8} mole fraction of oxygen. This value supports qualitatively our statement mentioned earlier that the solubility of oxygen in liquid hydrogen should be less than 0.5 p.p.m. in this temperature region. According to the measurements of Petit[5]), the solubility of oxygen in liquid hydrogen would be less than 1 p.p.m.

The fact that solid oxygen is less soluble than solid nitrogen in liquid hydrogen is also consistent with the measurements on the solubility of solid oxygen and solid nitrogen in gaseous hydrogen at somewhat higher temperatures.[13])

REFERENCES

1) Dokoupil, Z., Van Soest, G. and Swenker, M. D. P., Commun. Kamerlingh Onnes Lab., Leiden No. 297; Appl. sci. Res. **A5** (1955) 182.
2) Verschoyle, T. T. H., Trans roy. Soc. London **A230** (1931) 189.
3) Ruhemann, M. and Zinn, N., Phys. Zd.U.S.S.R. **12** (1937) 389.
4) Steckel, F. and Zinn, N., Zhurn. khim. Prom. **16** (1939).
5) Petit, P., Comp. rend. **297** (1958) 1171.
6) Omar, M. H. and Dokoupil, Z., Commun. Leiden No. 330*a*; Physica **28** (1962) 33.
7) Tompkins, F. C. and Young, D. M., J. sci. Instrum. **27** (1950) 224.
8) Brilliantov, N. A. and Fradkov, A. B., J. techn. Phys. **27** (1957) 2405.
9) Hildebrand, J. H. and Scott, R. L., The solubility of non electrolytes (Reinhold Publ. Corp., New York 1950).
10) Schröder, J., Z. physik. Chem. (Leipzig) **11** (1893) 449.
11) Giauque, W. F. and Clayton, J. O., J. amer. chem. Soc. **55** (1933) 4875.
12) Din, F., Thermodynamic functions of gases III (Butterworths, London 1961).
13) Dokoupil, Z., Progress in Low Temperature Physics, edited by C. J. Gorter. (North-Holland Publishing Company, Amsterdam, 1961). Vol. III chapt. XI.

ACKNOWLEDGEMENTS

I am grateful to Prof. C. J. Gorter who has given me the opportunity to study in the Kamerlingh Onnes Laboratory. I am indebted to my promotor Prof. K. W. Taconis for his continuous stimulation and helpful suggestions while supervising this research.

I wish to express my gratitude to Dr. Z. Dokoupil who introduced me to phase-equilibria at low temperature, for his daily discussions, continual interest and help.

My thanks are due to Miss H. G. M. Schroten for her assistance; to Dr. W. Duffy for reading the text and improving the language. The invaluable assistance of many members of the technical staff of the Kamerlingh Onnes Laboratory is greatly appreciated.

I should like to use this opportunity to express my thanks to the authorities of the Kamerlingh Onnes Laboratory and Leiden University for their generous hospitality.

My thanks are due to the authorities of the Faculty of Science of the Assyout University, Egypt, U.A.R., for extending my mission in The Netherlands to enable me to complete this thesis.

SAMENVATTING

Dit proefschrift heeft tot onderwerp het fasenevenwicht van binaire mengsels bij lage temperaturen.

In hoofdstuk I worden metingen van het *damp-vloeistof* evenwicht van het systeem H_2–N_2 besproken.

Met behulp van de stromingsmethode is de dauwlijn gemeten in het temperatuurgebied van 63 tot 75°K en bij drukken tussen 5 en 45 atm. Voor de lagere drukken is een extrapolatiemethode uitgewerkt. Hiermede zijn de tot nu toe ontbrekende gegevens van dit systeem aangevuld. De verkregen dauwlijn en de gebruikte kooklijn worden thermodynamisch onderzocht op hun interne samenhang.

Hoofdstuk II behandelt het evenwicht tussen de *vaste en de vloeibare* fase van het systeem N_2–CH_4. Met behulp van de dampspanningsmetingen en van de calorische methoden zijn de vloeistoflijn, de smeltlijn en de driefasen lijn van het systeem bepaald. Beide componenten blijken gedeeltelijk oplosbaar te zijn in de vaste fase. Het smeltdiagram behoort tot het eutectische type. De eutectische samenstelling bevat 23.8% methaan en de stikstof kan tot maximaal 45% opgelost worden in het kristalrooster van methaan. De smelttemperaturen van mengsels met een concentratie kleiner dan 23% methaan liggen dicht bij de eutectische temperatuur van 62.6°K. Enkele metingen betreffende het evenwicht tussen beide vaste fasen voltooien enigszins het beeld bij nog lagere temperaturen. Uit de beschikbare gegevens van dit systeem is het driedimensionale fasenmodel afgeleid boven 63°K bij drukken kleiner dan 2 atm. Met behulp van de theorie van de reguliere mengsels is de thermodynamische analyse uitgevoerd.

Een ander type fase evenwicht wordt in hoofdstuk III behandeld: het evenwicht tussen de *gas en de vaste* fase van het O_2–H_2 systeem. De resultaten zijn verkregen met behulp van de aan dit systeem aangepaste stromingsmethode en bevestigen de berekende oplosbaarheden beneden de triplepuntstemperatuur van zuurstof bij drukken van 5, 10 en 15 atm.

Het evenwicht tussen de *zuivere vaste* fase en de *vloeibare* fase is beschreven in hoofdstuk IV. Met behulp van de statische methode is de oplosbaarheid van vaste stikstof of zuurstof in vloeibare waterstof beneden de kritische temperatuur van waterstof onderzocht. De nauwkeurigheid van het gebruikte analyse apparaat beperkt het onderzoek tot temperaturen boven 27°K voor het systeem N_2–H_2. De geëxtrapoleerde waarde voor de oplosbaarheid van N_2 in vloeibare waterstof bij het kookpunt is $10^{-6}\%$. In het O_2–H_2 systeem is geen meetbare oplosbaarheid gevonden in hetzelfde p–T gebied. De meetresultaten zijn met behulp van de theorie van Hildebrand geanalyseerd.

gebruikte analyse apparaat beperkt het onderzoek tot temperaturen boven 27°K voor het systeem N_2-H_2. De geëxtrapoleerde waarde voor de oplosbaarheid van N_2 in vloeibare waterstof bij het kookpunt is 10^{-8}%. In het O_2-H_2 systeem is geen meetbare oplosbaarheid gevonden in hetzelfde p-T gebied. De meetresultaten zijn met behulp van de theorie van Hildebrand geanalyseerd.

SAMENVATTING

Dit proefschrift heeft tot onderwerp het fasenevenwicht van binaire mengsels bij lage temperaturen.

In hoofdstuk I worden metingen van het damp-vloeistof evenwicht van het systeem H_2-N_2 besproken.

Met behulp van de stromingsmethode is de dauwlijn gemeten in het temperatuurgebied van 62 tot 77°K en bij drukken tussen 5 en 45 atm. Voor de lagere drukken is een extrapolatiemethode uitgewerkt. Hiermede zijn de tot nu toe ontbrekende gegevens van dit systeem aangevuld. De verkregen dauwlijn en de gebruikte kooklijn werden thermodynamisch onderzocht op hun interne samenhang.

Hoofdstuk II behandelt het evenwicht tussen de vaste en de vloeibare fase van het systeem N_2-CH_4. Met behulp van de dampspanningsmetingen en van de calorische methoden zijn de vloeistoflijn, de smeltlijn en de driefasenlijn van het systeem bepaald. Beide componenten blijken gedeeltelijk oplosbaar te zijn in de vaste fase. Het smeltdiagram behoort tot het eutectische type. De eutectische samenstelling bevat 23.3% methaan en de stikstof kan tot maximaal 45% opgelost worden in het kristalrooster van methaan. De smelttemperaturen van mengsels met een concentratie kleiner dan 23% methaan liggen dicht bij de eutectische temperatuur van 62.6°K. Enkele metingen betreffende het evenwicht tussen beide vaste fasen vertonen enigszins het beeld bij nog lagere temperaturen. Uit de beschikbare gegevens van dit systeem is het driedimensionale fasenmodel afgeleid boven 63°K bij drukken kleiner dan 2 atm. Met behulp van de theorie van de reguliere mengsels is de thermodynamische analyse uitgevoerd.

Een ander type fase evenwicht wordt in hoofdstuk III behandeld: het evenwicht tussen de gas en de vaste fase van het O_2-H_2 systeem. De resultaten zijn verkregen met behulp van de aan dit systeem aangepaste stromingsmethode en bevestigen de berekende oplosbaarheden beneden de tripelpuntstemperatuur van zuurstof bij drukken van 5, 10 en 15 atm.

Het evenwicht tussen de zuivere vaste fase en de vloeibare fase is beschreven in hoofdstuk IV. Met behulp van de analytische methode is de oplosbaarheid van vaste stikstof of zuurstof in vloeibare waterstof beneden de kritische temperatuur van waterstof onderzocht. De geringe gevoeligheid van het